TRANSFORM CODING TECHNIQUES

AND

THEIR APPLICATIONS IN JPEG SCHEME

A Thesis

Submitted to

The Department of Electronic Engineering

of

The Chinese University of Hong Kong

In

Partial Fulfilment of the Requirements

for the Degree of

Master of Philosophy

By

Chun-tat SEE

June, 1991

ACKNOWLEDGEMENT

I would like to express my gratitude to my supervisor, Dr. W.K.CHAM, for his invaluable advice, comments and sharing of his experience during the past years of my research study, and also his patience in reading all manuscripts and the thesis.

Also, I would like to thank all my colleagues for their help and discussion during the course of this research.

Finally, I wish to give my special and deepest gratitude to my wife, Hedy, for her support and encouragement throughout the whole period of this research study.

ABSTRACT

Transform coding of image has been used extensively in recent years for data compression. In this thesis, some techniques and parameters will be considered and discussed. With the introduction of an international standard, the JPEG scheme, we will study its coding methods and use some techniques to improve the coding performance.

The heart of a transform coding system is the transform used. The Discrete Cosine Transform (DCT) is usually employed because of its near optimum performance. On the other hand, dyadic symmetry has been used successfully in generating new transforms with simpler implementation and close performance to DCT and the technique has been used to generate the Dyadic Matrices [CHAM90]. In this thesis, it will be proved that the maximum size of Dyadic Matrices is 8 only. The relationship between destroying dyadic symmetry and application of Dyadic Matrices in generating orthogonal transforms will be given.

In a conventional transform coding system, DC and AC coefficients are quantized and bits are allocated and sent to receiver. The bits needed in coding the DC coefficients can be saved by DC restoration scheme and allocated to AC coefficients for more precise coding. This method will be extended that not only the DC coefficients, but also some low sequency coefficients will be truncated according to the activity of image blocks. At the receiver, these truncated low sequency coefficients are estimated to reconstruct the image. Simulation results will be given to compare the performance with the Chen & Smith (C&S) [CHENs77] scheme.

Block size is another parameter that affects the performance of a transform coding system. Variable block size techniques have been used for enhancing coding performance [VAISEg87] [CHEN89]. In this thesis, an Edge Discriminator is proposed which is used

to determine the block size. Simulation using real images has shown that a variable block size coding system using the proposed discriminator has better performance over that of [CHEN89].

A JPEG scheme [JPEG90] is recently proposed for still image compression. It utilizes the techniques of transform coding and DPCM coding. As the JPEG scheme will become an international standard, further improvement should be based on it for compatibility. In this thesis, the basic JPEG scheme is described and two techniques are used to enhance its performance. One is by the use of a Minimum Edge Difference (MED) predictor and the other is by the use of variable block size technique. Simulation results have shown that both techniques can improve the performance of the basic JPEG scheme.

NOTATIONS

DCT	Discrete cosine transform
KLT	Karhunen-Loeve transform
MSE	Mean square error
BRE	Basis restriction error
MRB	Maximum reducible bit
TE	Transform efficiency
F	Field
S	Dyadic symmetry
bpp	Bit per pixel
N	Dimension of a matrix or a vector
ρ	Adjacent element correlation coefficient
σ^2	Variance
*	'Logical and'
$\oplus$	'Exclusive or' (i.e. binary two addition)
[T]	A matrix or a transform T
$\vec{T}(i)$	i^{th} Basis vector of [T]
t(*N*,i,j)	$(i,j)^{th}$ element of a order-N [T] (N is included only when needed)
$[\ ]^t$	Transpose
$[C_x]$	Covariance matrix of X
E[.]	Expected value of the variable in [ ]
$\vec{x}$	Vector in spatial domain
$[H_s(N)]$	Sequency-ordered Walsh transform matrix
$[H_n(N)]$	Natural-ordered Walsh transfor matrix

$\vec{i}$	A vector in field F representing i
(i,m)	m^{th} bit in $\vec{i}$
U(i)	Dyadic shift for i^{th} basis vector in a matrix
$\vec{U}(i)$	A vector in field F representing U(i)
U(i,m)	m^{th} bit in $\vec{U}(i)$

TABLE OF CONTENTS

1. INTRODUCTION

1.1 Introduction

Over the past two decades, with the continuing development of the modern communication and computer technologies, the demand for storage and transmission of image data is greatly increasing. Yet, images represent a large amount of information. For example, a monochrome image of 512 x 512 pels and resolution of 8 bits/pel requires 2 Megabits for representation. This requirement increases threefold for a colour image. Due to the limitations of the memory for storage and the channel capacity for transmission, compression of image data is necessary.

Different data compression methods have been proposed to compress the image data to as low a bit rate as possible, while the image fidelity should be kept reasonably good [NETRA180] [JAIN81] [JAIN89]. Predictive coding and transform coding are two commonly used methods. In predictive coding, the redundancy of image data in spatial domain is exploited and removed. It has the advantage of simple implementation, but the compression ability is not very high. Transform coding is a method that transform a block of image data into a transform domain, trying to reduce the correlation between the image data. The compression ability of transform coding is very high but its computational requirement is relatively larger. With the advances in hardware technologies, this computational burden is greatly relieved and the compression ability becomes the more important concern. Therefore, many image coding standards and proposals [JPEG90] [ELSEV90] [JURGE91] adopt transform coding. In this thesis, we will present our investigation results on three aspects of a transform coding system, which are transformation, bit allocation and block size.

With maturity and vast amount of research work devoted to image coding techniques, a committee under the International Telegraph and Telephone Consultative Committee (CCITT) and International Standards Organization (ISO) called Joint Photographic Expert Group (JPEG),

is drafting a still image coding scheme. This scheme, which is basically a transform coding system, is intended to be used as an international standard. We expect that this standard will play a dominant role in image coding system. For example, there is already a processor in the industry that employs the JPEG scheme [CUBE90]. To maintain easy upgradability and compatibility, further enhancement should therefore be made on the basis of the JPEG scheme. In this thesis, we will study and propose two techniques to enhance the performance of the basic JPEG scheme. One is by the use of a more efficient predictor for DC coefficient and the other is by variable block size technique.

1.2 A Basic Transform Coding System

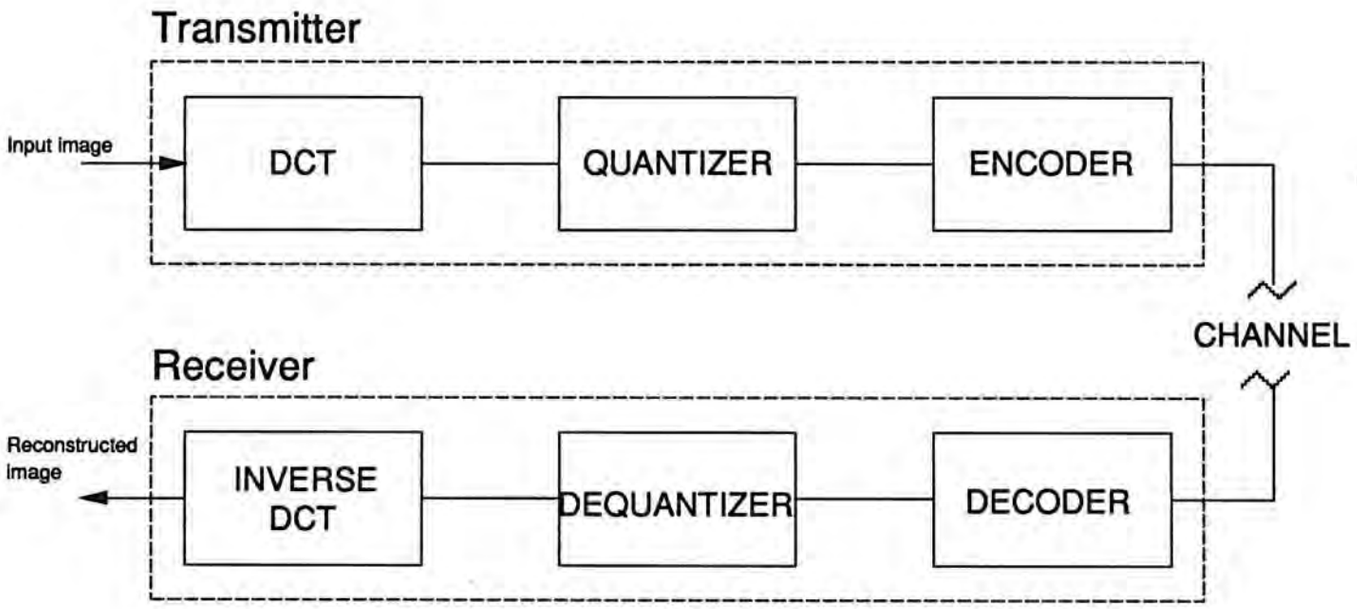

Fig.1.1 Block diagram of a transform coding system

Fig.1.1 shows the functional block diagram of a basic transform coding system. At the transmitter, an input image is first divided into square blocks of size NxN. Each block will go through an orthogonal transform. The transform coefficients are then quantized and the

quantized coefficients are encoded. At the receiver, the received data are similarly decoded and dequantized to obtain the transform coefficients. Finally, an inverse transform is applied to reconstruct the image in spatial domain.

In the basic transform coding system, there are three basic parameters which can affect the coding performance :

a. Choice of Transform

A transform is said to be optimum if it has the highest energy packing ability. It has been shown that the Karhunen Loeve Transform (KLT) can achieve this target. However, as the basis vectors of KLT are the eigenvectors of the covariance matrix of an image, the KLT is signal dependent. For different images, computation is needed to find the corresponding KLT in order to achieve the theoretically optimum performance. Moreover, there is no fast computational algorithm for computing the transform coefficients. Hence the KLT is seldom used. Instead, the Discrete Cosine Transform (DCT) is usually employed because of its near optimum performance and existence of fast computational algorithm.

Although DCT is so far reported to be the best suboptimum transform, many researchers are continuing to find if there are still better transforms. For example, CHAM has proposed a High Correlation Transform (HCT), Low Correlation Transform (LCT) [CHAMc86] and families of Integer Cosine Transform (ICT) [CHAM89] [CHAMc91], by using a concept of Dyadic Symmetry. The technique has been used to generate a family of Dyadic Matrix [CHAM90]. In this thesis, we will study the formation of these Dyadic Matrices and prove that the maximum size of Dyadic Matrix is 8. Relationship between destroying dyadic symmetry and Dyadic Matrix and application of using Dyadic Matrices in generating orthogonal matrices will be given. The details will be described in chapter 2.

b. Quantization

DC coefficients and AC coefficients have different characteristics and so are usually treated differently. It has been found that most two-dimensional transformations produce Laplacian distributed AC transform coefficients [REINIg83]. Hence, Max's quantizer [MAX60] with probability distribution of coefficients assumed to be Laplacian can be used to quantize the transform coefficients. By making use of these quantizers, the reconstructed image should have minimum distortion in terms of Mean Square Error (MSE). Moreover, a further improvement of picture quality is possible by taking into account of human visual sensitivity. As human visual system responses differently for error in different coefficients, the characteristic of quantizer should therefore be designed accordingly. This approach has been adopted by [NGANls89] [JPEG90].

DC coefficients have no specific distribution and contain information about the brightness. It is usually quantized uniformly with a fixed number of bits (e.g. 8 bits), independent of its variance. This fixed bit allocation for DC coefficients can consume a large percentage of bits available, particularly at low bit rate. However, CHAM has proposed that the DC coefficients could be truncated [CHAMc84]. By this way, no bit is needed for sending the DC coefficients and more bits can be allocated to AC coefficients for more precise coding. At receiver, the DC coefficients can be estimated by using three DC coefficient estimation schemes. In this thesis, this method will be further studied to reduce bit rate. In a proposed Low Sequency Coefficient Truncation scheme, not only the DC coefficients, but also some low sequency coefficients are truncated.

c. Block Size

In a conventional transform coding system, the block size N used to partition an image is fixed. The commonly used block sizes are 8x8 or 16x16. However, this approach has not

taken the advantage of larger bit rate reduction using larger N for areas with little changes, and better visual quality using smaller N for areas with high activities. In this thesis, we will present our results using the variable block size technique for performance improvement. An Edge Discriminator will be proposed to determine the block size.

1.3 Thesis Organization

For the rest of the thesis, chapter 2 will first study the formation of orthogonal Dyadic Matrices and the maximum size of Dyadic Matrix will be proved. The relationship between destroying dyadic symmetry and Dyadic matrix as well as application of Dyadic Matrices in generating orthogonal transform are also discussed. In chapter 3, the method of Low Sequency Coefficient Truncation (LSCT) is presented. The first LSCT scheme is based on the C&S scheme [CHENs77] and some low sequency coefficients are truncated and estimated according to the class of blocks concerned. Then a second LSCT scheme is proposed, trying to eliminate the defect of LSCT 1. Simulation results are given and conclusions are drawn. In chapter 4, the Variable Block Size (VBS) technique is studied and by using an Edge Discriminator, an enhanced version of VBS system with respect to a Chen's system is proposed. Simulation will be given to compare their performance.

In chapter 5, the basic JPEG scheme will be described. Two techniques will be used, hoping to enhance the performance of basic JPEG scheme. Firstly, a more efficient Minimum Edge Difference (MED) predictor will be used for encoding DC coefficients. The other is by the use of variable block size technique. Simulation result will also be given to show how to obtain improved performance. This thesis concludes with chapter 6, which collates the discoveries and research work performed during the research programme, and makes suggestions on potential areas for further research.

2. DYADIC MATRICES AND THEIR APPLICATIONS

2.1 Introduction

In a transform coding system, an orthogonal transform is required for transforming images from spatial domain to transform domain. The transform should compact energy of an image to as few low sequency transform coefficients as possible to improve the Mean Square Error performance of the coding system. Furthermore, the transform should also possess fast computational algorithm and simple hardware structure for easy implementation. The optimum transform that has the highest energy compaction ability is the KLT. However, it is rarely used in practice because it does not possess fast computational algorithm and is signal dependent. Thus, other suboptimum transforms, such as Fourier Transform [ANDREp68], Walsh Transform (WT) [PRATTk69], the DCT [AHMEDtr74], KLT [AHMEDr75], High Correlation Transform (HCT), Low Correlation Transform (LCT) [CHAMc86] and Integer Cosine Transform (ICT) [CHAMc89], were proposed to achieve one or all of the targets. Among these suboptimum transforms, the DCT is found to have the best performance and possess fast computational algorithm. However, it requires real arithmetic and so its implementation is complex.

On the other hand, the WT has only '1' and '-1' as its elements requiring only addition and subtraction operations and so can be easily implemented. However, its energy compaction ability does not perform well enough in comparison to the DCT. To compromise between computational complexity and transform performance, new transforms were proposed. For example, HCT and LCT which were derived using the concept of Dyadic Symmetry [CHAMc86] have improved transform performance and virtually the same computational requirement as the WT. A series of new transforms, called Integer Cosine

Transform (ICT), has also recently been generated [CHAM89] [CHAMc91] by using dyadic symmetry, which possesses about the same performance as the DCT but involves integer arithmetic only.

In the development of HCT and LCT using Dyadic Symmetry, the structure of WT kernel was modified to approximate the DCT for image coding. This technique for generating HCT and LCT has been used to generate a family of orthogonal matrices, called Dyadic Matrix, from WT [CHAM90]. The kernel components of these Dyadic Matrices can have arbitrary values and hence they may found applications in different areas. In this chapter, we are going to prove that the maximum size of Dyadic Matrix is 8. The application of Dyadic Matrices in generating new transform for image coding is also demonstrated and components of the transform for optimum performance are found.

In section 2.2.1, the basic definitions of dyadic shift, dyadic symmetry and Dyadic Matrix will be given. By examinating in detail how the Dyadic Matrix is generated, we prove in section 2.2.2 that the maximum size of Dyadic Matrix is 8. In section 2.3.1, the performance criteria used for transform performance evaluation will be defined. In section 2.3.2 - 2.3.3, two transform structures will be proposed using the Dyadic Matrix and the components for optimum transform performance are found. Comparison is made by using the performance criteria defined. Finally, conclusion will be drawn in section 2.4.

2.2 Theory of Dyadic Matrix

Consider a 4x4 matrix [A] :

$$[A] = \begin{bmatrix} a_0 & a_1 & a_2 & a_3 \\ a_3 & a_2 & -a_1 & -a_0 \\ a_2 & -a_3 & -a_0 & a_1 \\ a_1 & -a_0 & a_3 & -a_2 \end{bmatrix}$$

[A] is a Dyadic Matrix. It can be observed that [A] is always orthogonal whatever values a_0, a_1, a_2 and a_3 assume. The 1st, 2nd and 3rd basis vectors of matrix [A] are obtained by applying 3rd, 2nd and 1st dyadic shift to the 0th basis vector respectively. The resulting matrix is orthogonal and possesses the same sign distribution of WT. It has been found that there are two Dyadic Matrices for order-4 and eight Dyadic Matrices for order-8. These Dyadic Matrices have the property that each basis vector can be obtained by a Dyadic Shift operation of other basis vector and magnitude of the N components in the transform kernel can be set arbitrary. Thus, the choice of a Dyadic Matrix and kernel components can be set according to different applications, not only limited to that of substituting DCT in transform coding. In section 2.2.2, we shall prove that the maximum size of Dyadic Matrix is only 8. In order to have a complete understanding of the Dyadic Matrices, the Dyadic Shift, Dyadic Symmetry and Dyadic Matrix will be first defined as follow :

2.2.1 Basic Definition [CHAMc86]

Definition 2.1 :

A vector of 2^m elements $[a_0, a_1, \ldots, a_{2^m-1}]$, where m is an positive integer, is said to have a S^{th} dyadic symmetry (DS) if and only if

$$a_j = c \cdot a_{j \oplus s} \tag{2.1}$$

where (i) $\oplus$ is 'exclusive or', (ii) j is an integer in the range $[0,2^m-1]$ and S is an integer in the range $[1,2^m-1]$, and (iii) $c = 1$ when the symmetry is even and $c = -1$ when the symmetry is odd.

Definition 2.2 :

Vectors $[a_0, a_1, \ldots, a_{2^m-1}]$ and $[b_0, b_1, \ldots, b_{2^m-1}]$ are said to have the common DS S if

$$a_j = c \cdot a_{j \oplus s} \tag{2.2a}$$

$$b_j = d \cdot b_{j \oplus s} \tag{2.2b}$$

where c and d can be 1 or -1.

The two vectors are said to have same DS if c and d are equal, otherwise they are said to have opposite DS. It has been shown that two vectors having opposite DS are orthogonal to each other.

Let F be a binary field, which has '0' and '1' as its elements, and 'logical and' {*} and 'exclusive or' {⊕} as its operations. For a vector with 2^m elements over a number field, there can be 2^m-1 DSs. These DSs can be represented as vectors in F. Unless specified otherwise, vectors in the field F are column vectors. For example, a 7^{th} DS in a order-8 vector can be represented as $[1\ 1\ 1]^t$.

Definition 2.3 :

The r DSs $\vec{S}_1, \vec{S}_2, \ldots, \vec{S}_r$ are said to be dependent if there exist r elements $k_1, k_2, \ldots, k_r$, not all zero, such that

$$k_1 \cdot \vec{S}_1 \oplus k_2 \cdot \vec{S}_2 \oplus \cdots \oplus k_r \cdot \vec{S}_r = 0 \tag{2.3}$$

Otherwise, the r dyadic symmetries are said to be independent.

Definition 2.4 :

Let $\vec{A}$ be a vector with 2^m elements a_i and has dyadic symmetry S. If the vector is replaced by another vector $\vec{A}'$ with same sign distribution but lacking the S^{th} dyadic symmetry, then the S^{th} dyadic symmetry in the vector $\vec{A}$ is said to be destroyed.

From [CHAMc86], every basis vector of the WT contains all dyadic symmetries. For example, if $\vec{A}$ is the 1st basis vector of sequency-ordered order-8 WT and is replaced by vector $\vec{A}$', in which the 7th dyadic symmetry destroyed, then :

$$\vec{A} = [1 \quad 1 \quad 1 \quad 1 \quad -1 \quad -1 \quad -1 \quad -1]$$

$$\vec{A}' = [b \quad b \quad b \quad b \quad -c \quad -c \quad -c \quad -c]$$

where b and c are not equal.

It should be noted that there are more than one way in which the DS of a vector may be destroyed. In the above example, $\vec{A}$' can also be [b b c c -b -b -c -c] or [b c b c -b -c -b -c]. To maintain orthogonality of the transform matrix, a pairs of WT basis vectors having common DS should be replaced each time a dyadic symmetry is destroyed. The components of new vectors can be set arbitrary but the orthogonality of the matrix is still maintained. Therefore, destroying dyadic symmetry allows new transforms with arbitrary components to be generated. By using this technique, two transforms, called HCT and LCT, have been generated [CHAMc86].

Definition 2.5 :

Let $\vec{A}$ be a vector of $[a_0, a_1, \ldots, a_{N-1}]$. A vector $\vec{A}$' is said to be obtained by a Dyadic Shift U from $\vec{A}$ if the elements of $\vec{A}$' are :

$$a'_j = a_{j \oplus U} \tag{2.5}$$

where $j \in [0,N-1]$, $U \in [0,N-1]$.

Let $[H_n(N)]$ be an order-N natural-ordered Walsh Matrix with elements h(i,j), where $N = 2^m$, m is an positive integer and i,j are row and column indices of $[H_n(N)]$ respectively. For simplicity, the order of a matrix or vector which is denoted as N will be omitted usually.

When there is a need in specifying the order, it will be indicated by number or notation in italics. An order-N natural-ordered Dyadic Matrix is defined from $[H_n(N)]$ [CHAM90]. The definition of Dyadic Matrix is given below :

Definition 2.6 :

For an order-N matrix $[T(N)]$, where $N = 2^m$ and m is a non-zero positive integer, let t(i,j) and $\vec{T}(i)$ represent its $(i,j)^{th}$ element and i^{th} basis vector respectively. $[T(N)]$ is said to be a Dyadic Matrix if

$$t(i,j) = \begin{cases} t(0,j) & , \text{ if } i = 0 \\ h(i,j) \cdot t(0, j \oplus U(i)) & , \text{ if } i \in [1,N-1] \end{cases} \tag{2.5}$$

where $j \in [0,N-1]$, U(i) is the dyadic shift for i^{th} basis vector and in the range [1,N-1], and $\oplus$ is the 'exclusive-or' operator.

By the definition of Dyadic Matrix, it can be seen that given the N elements t(0,j) of the 0^{th} basis vector, $\vec{T}(i)$ can be obtained by a dyadic shift U(i) applied to $\vec{T}(0)$ and then weighted by the i^{th} basis vector $\vec{H_n}(N,i)$ of natural-ordered Walsh matrix. Indeed, the weighting of $\vec{T}(i)$ by $\vec{H_n}(N,i)$ determines the sign of t(i,j) only. Therefore, $\vec{T}(i)$ is said to be obtained by *sign weighted dyadic shift U(i).*

By applying different sets of U(i), many Dyadic Matrices can be obtained. Among these matrices, only those matrices which are orthogonal are of our interest. Let $\vec{i}$ be a vector over F representing i and $\vec{U}(i)$ be a vector over F representing dyadic shift U(i) for i^{th} basis vector. It has been shown that [CHAM90] if $\vec{T}(i)$ and $\vec{T}(k)$ are obtained from $\vec{T}(0)$ by sign weighted dyadic shift U(i) and U(k) respectively, where $i \neq k$, then $\vec{T}(i)$ and $\vec{T}(k)$ are orthogonal if the following condition is satisfied :

$$\vec{U}^t(i) \cdot \vec{k} \oplus \vec{U}^t(k) \cdot \vec{i} = 1 \tag{2.6}$$

Moreover, $\vec{U}(i)$ and $\vec{U}(k)$ should not be equal and satisfy the condition :

$$\vec{U}^{t}(i)\cdot i = 1 \qquad (2.7a)$$

$$\vec{U}^{t}(k)\cdot k = 1 \qquad (2.7b)$$

For a Dyadic Matrix to be orthogonal, eq.(2.6) & (2.7) have to be satisfied for every pairs of basis vector $\vec{T}(i)$ and $\vec{T}(k)$. Computer program has been used to search for dyadic shift U(i) for each basis vector such that the resulting Dyadic Matrix is orthogonal. For N = 2, 4, 8, the results are summarized as follow :

For N = 2 :

	i		
	0	1	
Dyadic shift U(i)	0	1	--- $DM_0(2)$

For N = 4 :

	i				
	0	1	2	3	
Dyadic shift U(i)	0	1	3	2	--- $DM_1(4)$
	0	3	2	1	--- $DM_2(4)$

For N = 8 :

	i								
	0	1	2	3	4	5	6	7	
Dyadic shift U(i)	0	1	3	6	7	4	5	2	--- $DM_3(8)$
	0	1	7	2	5	6	3	4	--- $DM_4(8)$
	0	3	2	5	7	6	4	1	--- $DM_5(8)$
	0	3	6	1	5	4	2	7	--- $DM_6(8)$
	0	5	3	2	6	1	4	7	--- $DM_7(8)$
	0	5	7	6	4	3	2	1	--- $DM_8(8)$
	0	7	2	1	6	3	5	4	--- $DM_9(8)$
	0	7	6	5	4	1	3	2	--- $DM_{10}(8)$

where, for later reference, DM_i are names given to those matrices obtained by applying the set of dyadic shift to corresponding basis vectors.

The results of Dyadic Matrix mentioned above have been reported in [CHAM90]. To find higher order Dyadic Matrix ($N \geq 16$), similar procedure can be used. However, we shall prove that there is no combination of dyadic shift which can be applied for generating orthogonal Dyadic Matrix with order greater than 8.

2.2.2 Maximum Size of Dyadic Matrix

To find an order-N orthogonal Dyadic Matrix, we have to find dyadic shift $\vec{U}(i)$ for the i^{th} basis vector, i = 1,2,...,N-1, satisfying eq.(2.6) & eq.(2.7). The conditions of orthogonality in eq.(2.6) & eq.(2.7) can be expanded into eq.(2.8a) and eq(2.8b).

$$\begin{bmatrix} \vec{U}(1)\cdot\vec{1} & & & \\ & \vec{U}(2)\cdot\vec{2} & & \\ & & \ddots & \\ & & & \vec{U}(N)\cdot\vec{N} \end{bmatrix} = \begin{bmatrix} 1 \\ \vdots \\ 1 \end{bmatrix} \tag{2.8a}$$

$$\begin{bmatrix} \vec{U}(1)\cdot\vec{2} \oplus \vec{U}(2)\cdot\vec{1} & & & & & & \\ \vec{U}(1)\cdot\vec{3} \oplus & & \vec{U}(3)\cdot\vec{1} & & & & \\ \vdots & \vdots & & \ddots & & & \\ \vec{U}(1)\cdot\vec{N} \oplus & & & & & & \vec{U}(N)\cdot\vec{1} \\ & \vec{U}(2)\cdot\vec{3} \oplus & & \vec{U}(3)\cdot\vec{2} & & & \\ & \vec{U}(2)\cdot\vec{4} \oplus & & & \vec{U}(4)\cdot\vec{2} & & \\ & & & & & \ddots & \\ & & & & & \vec{U}(N-2)\cdot\overrightarrow{(N-1)} \oplus & \vec{U}(N-1)\cdot\overrightarrow{(N-2)} \end{bmatrix} = \begin{bmatrix} 1 \\ \vdots \\ 1 \end{bmatrix}$$

(2.8b)

Let $\vec{U}(i)$ and $\vec{i}$ be

$$\vec{U}(i) = [U(i,1) \quad U(i,2) \quad \ldots \quad U(i,m)]^t$$

$$\vec{i} = [i(1) \quad i(2) \quad \ldots \quad i(m)]^t$$

where $m = \log_2 N$, U(i,1) and i(1) are the most significant bit of $\vec{U}(i)$ and $\vec{i}$ respectively.

Hence,

$$\vec{U}(i)\cdot\vec{k} \oplus \vec{U}(k)\cdot\vec{i} =$$

$$\{U(i,1)\cdot k(1) \oplus U(i,2)\cdot k(2) \oplus \ldots \oplus U(i,m)\cdot k(m)\} \oplus \{U(k,1)\cdot i(1) \oplus U(k,2)\cdot i(2) \oplus \ldots \oplus U(k,m)\cdot i(m)\}$$

(2.9)

Eq.(2.8a) and (2.8b) can be combined and expressed as :

$$\begin{bmatrix} (1,1) & \cdots & (1,m) & & & & & & & & & & & & \\ & & & (2,1) & \cdots & (2,m) & & & & & & & & & \\ (2,1) & \cdots & (2,m) & (1,1) & \cdots & (1,m) & & & & & & & & & \\ & & & & & & (3,1) & \cdots & (3,m) & & & & & & \\ (3,1) & \cdots & (3,m) & & & & (1,1) & \cdots & (1,m) & & & & & & \\ & & & (3,1) & \cdots & (3,m) & (2,1) & \cdots & (2,m) & & & & & & \\ \vdots & & & & & & & \cdots & & & & & & & \\ \vdots & & \ddots & & & & & \cdots & & & & & & & \\ & & & & & & & & & (N-1,1) & \cdots & (N-1,m) & & & \\ (N-1,1) & \cdots & (N-1,m) & & & & & & & (1,1) & \cdots & (1,m) & & & \\ & & & \cdots & & & & & & & \vdots & & & & \\ & & & & & & (N-1,1) & \cdots & (N-1,m) & (N-2,1) & \cdots & (N-2,m) & & & \end{bmatrix} * \begin{bmatrix} U(1,1) \\ U(1,2) \\ \vdots \\ U(1,m) \\ U(2,1) \\ \vdots \\ U(2,m) \\ \vdots \\ \vdots \\ U(N-1,1) \\ \vdots \\ U(N-1,m) \end{bmatrix} = \begin{bmatrix} 1 \\ \\ \\ \\ \\ \\ \\ \\ \\ \\ \\ 1 \end{bmatrix}$$

(2.10)

For example, when N = 4, eq.(2.10) becomes :

$$\begin{bmatrix} 0 & 1 & 0 & 0 & 0 & 0 \\ 0 & 0 & 1 & 0 & 0 & 0 \\ 1 & 0 & 0 & 1 & 0 & 0 \\ 0 & 0 & 0 & 0 & 1 & 1 \\ 1 & 1 & 0 & 0 & 0 & 1 \\ 0 & 0 & 1 & 1 & 1 & 0 \end{bmatrix} \cdot \begin{bmatrix} U(1,1) \\ U(1,2) \\ U(2,1) \\ U(2,2) \\ U(3,1) \\ U(3,2) \end{bmatrix} = \begin{bmatrix} 1 \\ 1 \\ 1 \\ 1 \\ 1 \\ 1 \end{bmatrix} \qquad (2.11)$$

Solving eq.(2.11), we obtain dyadic shift U(i) for each basis vector. There are two solutions for N = 4 as follow :

$$[U(1,1) \quad U(1,2) \quad U(2,1) \quad U(2,2) \quad U(3,1) \quad U(3,2)] = \begin{cases} [0 & 1 & 1 & 1 & 1 & 0] \\ [1 & 1 & 1 & 0 & 0 & 1] \end{cases}$$

which corresponding to

		i		
		1	2	3
U(i)	1	1	3	2
	3	3	2	1

In other words, there are two combinations of dyadic shift which can be applied to generate order-4 orthogonal dyadic matrices. The corresponding orthogonal Dyadic Matrices are

$$\begin{bmatrix} a_0 & a_1 & a_2 & a_3 \\ a_1 & -a_0 & a_3 & -a_2 \\ a_3 & a_2 & -a_1 & -a_0 \\ a_2 & -a_3 & -a_0 & a_1 \end{bmatrix} \quad \text{and} \quad \begin{bmatrix} a_0 & a_1 & a_2 & a_3 \\ a_3 & -a_2 & a_1 & -a_0 \\ a_2 & a_3 & -a_0 & -a_1 \\ a_1 & -a_0 & -a_3 & a_2 \end{bmatrix}$$

where a_0, a_1, a_2 and a_3 can assume any value.

These two Dyadic Matrices are the same as those obtained in [CHAM90] but derived using a different approach.

Furthermore, the dyadic shift $\vec{U}(2N,i)$ for order-2N dyadic matrix can be obtained from dyadic shift $\vec{U}(N,i)$ for order-N dyadic matrix. As,

$$U(2N,i,1) = 0 \text{ for } i = 1,2,...,N-1$$

Therefore, from eq.(2.10), U(2*N*,i,l) for $i \in [1,N-1]$ and $l \in [2,m+1]$ have to satisfy the same condition as U(*N*,i,l) for $i \in [1,N-1]$ and $l \in [1,m]$. Thus, given U(*N*,i), we can solve for U(2*N*,i).

For example, one of the two dyadic shift combinations for N = 4 is given by

$$[U(4,1) \;\; U(4,2) \;\; U(4,3)] = [3 \;\; 2 \;\; 1]$$

From them, we obtain U(*8*) as follow :

$$[U(8,1)\ \ U(8,2)\ \ U(8,3)\ \ U(8,4)\ \ U(8,5)\ \ U(8,6)\ \ U(8,7)] = \begin{matrix}[3 & 2 & 5 & 7 & 6 & 4 & 1]\\ [7 & 2 & 1 & 6 & 3 & 5 & 4]\\ [3 & 6 & 1 & 5 & 4 & 2 & 7]\\ [7 & 6 & 5 & 4 & 1 & 3 & 2]\end{matrix}$$

Another dyadic shift combination for N = 4 is given by :

$$[U(4,1)\ \ U(4,2)\ \ U(4,3)] = [1\ \ 3\ \ 2]$$

The U(8) obtained is :

$$[U(8,1)\ \ U(8,2)\ \ U(8,3)\ \ U(8,4)\ \ U(8,5)\ \ U(8,6)\ \ U(8,7)] = \begin{matrix}[1 & 3 & 6 & 7 & 4 & 5 & 2]\\ [5 & 3 & 2 & 6 & 1 & 4 & 7]\\ [1 & 7 & 2 & 5 & 6 & 3 & 4]\\ [5 & 7 & 6 & 4 & 3 & 2 & 1]\end{matrix}$$

Thus we can obtain all U(*8*) combinations from U(*4*) combinations simply by computer search.

The next procedure is to find the solution U(*16*,i) for order-16 orthogonal Dyadic Matrix. However, it is found by applying the truth table technique to eq.(2.10) that in order to maintain orthogonality in order-16 Dyadic Matrix, U(*8*,2), U(*8*,4), U(*8*,6) have to satisfy conditions given in the following table :

U(*8*,2)	U(*8*,4)	U(*8*,6)
E.V.	E.V.	E.V.
E.V.	O.V.	O.V.
O.V.	E.V.	O.V.
O.V.	O.V.	E.V.

Table 2.1 Condition of U(*8*) for U(*16*) to be exist, where

E.V.: even in value, i.e. the least significant bit of U(*8*,i) is 0

O.V.: odd in value, i.e. the least significant bit of U(*8*,i) is 1

In other words, if both U(*8*,2) and U(*8*,4) are E.V., then U(*8*,6) has to be E.V.

Examining the dyadic shift combination for N = 8, we find that there is no combination of U(*8*) which can satisfy condition listed in Table 2.1. Thus no solution of U(*16*,i) satisfying eq.(2.10) can be found and hence there is no orthogonal Dyadic Matrix for N = 16.

Moreover, as U(*2N*,i) must at least satisfy the same conditions as U(*N*,i), U(*2N*,i) has no solution for $N \geq 8$ and no dyadic matrix can be found.

2.3 Application of Dyadic Matrix in Generating Orthogonal Transform

In this section, we will present examples on using the Dyadic Matrix to generate new orthogonal transforms for image coding. The optimum components of Dyadic Matrix will be searched. To compare the performance of the transform obtained, criteria used in evaluating the performance of a transform matrix are first defined.

2.3.1 Transform Performance Criteria

Assume that a N-dimensional vector $\vec{x}$ is a sample from an one-dimensional, zero-mean, unit-variance, first-order Markov process with adjacent element correlation ρ, and covariance matrix $[C_x]$, where

$$[C_x] = E[\vec{x} \cdot \vec{x}^t] = \begin{bmatrix} 1 & \rho & \rho^2 & \cdots\cdots & \rho^{N-2} & \rho^{N-1} \\ \rho & 1 & \rho & \cdots\cdots & \rho^{N-2} & \\ \cdot & \cdot & \cdot & \cdot & \cdot & \cdot \\ \cdot & \cdot & \cdot & \cdot & \cdot & \rho \\ \rho^{N-1} & \cdot & \cdot & \cdot & \rho & 1 \end{bmatrix} \tag{2.12}$$

where E[.] denotes the expected value. In other words, the $(i,j)^{th}$ element of $[C_x]$ is

$$C_x(i,j) = \rho^{|i-j|} \tag{2.13}$$

The covariance matrix $[C_y]$ of vector $\vec{y}$, where $\vec{y} = [T]\,\vec{x}$ is the transformed vector of $\vec{x}$ by transform [T], is given by

$$\begin{aligned} [C_y] &= E[\vec{y} \cdot \vec{y}^t] \\ &= [T] \cdot [C_x] \cdot [T]^t \\ &= \begin{bmatrix} s(0,0) & \cdots & s(0,N-1) \\ \cdot & \cdots & \cdot \\ \cdot & \cdots & \cdot \\ s(N-1,0) & \cdots & s(N-1,N-1) \end{bmatrix} \end{aligned} \tag{2.14}$$

The variance of the i^{th} transform coefficient is $E[y^2(i)] = \sigma^2(i) = s(i,i)$.

Three performance criteria, namely, transform efficiency (TE) [CLARK85], maximum reducible bit (MRB) [WANGh84] and basis restriction mean square error (BRMSE) [JAIN79], all defined on the $[C_y]$, will be used in comparing performance of different transforms. Their definitions are given as follow :

Definition 2.7 :

Transform efficiency (TE) is defined as,

$$TE = \frac{\sum_{i=0}^{N-1} |s(i,i)|}{\sum_{p=0}^{N-1}\sum_{q=0}^{N-1} |s(p,q)|} \times 100\% \qquad (2.15)$$

TE indicates the ability of [T] to transform $\vec{x}$ into a vector of $\vec{y}$ of uncorrelated elements. The greater is the TE, the greater is the decorrelation ability of the transform matrix [CLARK85]. TE of the optimum KLT is 100%.

Definition 2.8 :

The maximum reducible bit (MRB) is given as,

$$MRB = -\frac{1}{2N}\sum_{i=0}^{N-1} \log_2 \sigma^2(i)$$

$$= -\frac{1}{2N}\sum_{i=0}^{N-1} \log_2 s(i,i) \qquad (2.16)$$

[WANGh84] has shown that MRB is related to the rate distortion function. It measures the maximum bit reducible from each transform coefficient. The greater is the MRB, the more bits are reducible and the better is the transform.

Definition 2.9 :

The basis restriction mean square error (BRE(v)) is defined as follow :

$$BRE(v) = \frac{\sum_{i=v}^{N-1} \sigma^2(i)}{\sum_{i=0}^{N-1} \sigma^2(i)} \tag{2.17}$$

where v is the number of elements in the transformed vector that can have nonzero value and $v \in [0,N-1]$. The BRE(v), for any v, will hence vary with the transform used. The smaller is the BRE(v), the better is the transform matrix.

In [CHAM86] new orthogonal matrices can be generated from WT by destroying dyadic symmetry. Such method is, however, very different from conventional approach and so is difficult to comprehend. We now establish a relationship between destroying dyadic symmetry and Dyadic Matrix, which is then used to generate new transform using conventional matrix equation. A sequency-ordered Walsh matrix $[H_s(N)]$ can be represented as :

$$[H_s(N)] = [P(N)] \cdot [D(N)] \cdot [Q(N)] \tag{2.18}$$

where $[P(N)]$: a permutation matrix reordering the rows of a matrix.

$[Q(N)]$: an order-N matrix which combines lower order submatrix in $[D(N)]$ into order-N matrix by using some dyadic symmetries.

$[D(N)]$: a block diagonal matrix composed of submatrices $[A(r_l)]$ of order r_l, where $r_l = 2^k$, k is an integer and l is an index.

i.e.

$$[D(N)] = \text{Diag}([A(r_1)],[A(r_2)],...,[A(r_l)])$$

$$\sum_{i=1}^{l} r_i = N$$

For example, if the rows in $[H_s(8)]$ are permuted that the even number basis vectors are put into upper half and odd number basis vectors are put into lower half and the 7th dyadic symmetry is used in [Q(8)], eq.(2.18) becomes :

$$[H_s(8)] = \begin{bmatrix} 1&0&0&0&0&0&0&0\\ 0&0&1&0&0&0&0&0\\ 0&0&0&0&1&0&0&0\\ 0&0&0&0&0&0&1&0\\ 0&1&0&0&0&0&0&0\\ 0&0&0&1&0&0&0&0\\ 0&0&0&0&0&1&0&0\\ 0&0&0&0&0&0&0&1 \end{bmatrix} \cdot \begin{bmatrix} 1&1&1&1&0&0&0&0\\ 1&1&-1&-1&0&0&0&0\\ 1&-1&-1&1&0&0&0&0\\ 1&-1&1&-1&0&0&0&0\\ 0&0&0&0&1&1&1&1\\ 0&0&0&0&1&1&-1&-1\\ 0&0&0&0&1&-1&-1&1\\ 0&0&0&0&1&-1&1&-1 \end{bmatrix} \cdot \begin{bmatrix} 1&0&0&0&0&0&0&1\\ 0&1&0&0&0&0&1&0\\ 0&0&1&0&0&1&0&0\\ 0&0&0&1&1&0&0&0\\ 1&0&0&0&0&0&0&-1\\ 0&1&0&0&0&0&-1&0\\ 0&0&1&0&0&-1&0&0\\ 0&0&0&1&-1&0&0&0 \end{bmatrix}$$

$$= [P(8)] \cdot [D(8)] \cdot [Q(8)] \qquad (2.19)$$

where $[D(8)] = \text{Diag}([A(4)],[A(4)])$ and

$$[A(4)] = \begin{bmatrix} 1&1&1&1\\ 1&1&-1&-1\\ 1&-1&-1&1\\ 1&-1&1&-1 \end{bmatrix}$$

If we replace the [A(4)] in eq.(2.19) by order-4 dyadic matrix [DM(4)] such that

$$[D'(8)] = \text{Diag}([DM(4)],[DM(4)]) \qquad (2.20)$$

then a new orthogonal matrix [T(8)] can be obtained :

$$[T(8)] = [P(8)]\ [D'(8)]\ [Q(8)] \qquad (2.21)$$

We can see that the matrix obtained by replacing $[A(r_i)]$ in eq.(2.18) by $[DM(r_i)]$ is the same as the matrix obtained by destroying dyadic symmetry. As there may have different

Dyadic Matrices for each order, therefore, with same dyadic symmetries destroyed, different orthogonal matrices can be constructed by using different orthogonal Dyadic Matrices. As a result, Dyadic Matrices, beside themselves being orthogonal matrices, can be used to generate new orthogonal matrices of higher order.

Consider $\vec{y}$, the transformed signal vector, which is obtained by transforming a signal vector $\vec{x}$ by transform [T]. The transform coefficients y_i are the inner product of basis vectors $\vec{T}(i)$ in [T] and $\vec{x}$. Assume that the $\vec{T}(i)$ are arranged in ascending sequency order of i. Then a good transformation is said to be done if most of the signal energy is confined in as small low sequency transform coefficients as possible. A large magnitude of y_i will be obtained if the basis vector $\vec{T}(i)$ resemble the signal vector $\vec{X}$. Since in natural, image signal vector vary slowly, the basis vector of a good transform should then have similar feature. For example, low sequency basis vectors of the DCT change smoothly while those of the WT have sudden changes between positive and negative kernel components. The DCT thus packs more energy into low sequency transform coefficients than the WT does.

Consider an order-8 WT as shown in Table 2.2. If some dyadic symmetries are destroyed, by using some Dyadic Matrices, from some basis vectors $\vec{H}(i)$, then the basis vectors will have components which can be varied to construct required structure in basis vectors. If the components are set in such a way that the replaced vectors have more smooth change between components, a better transform matrix, in terms of its energy compaction ability, can be generated. As more energy should be compact to lower sequency transform coefficients, higher priority should be given to a basis vector of lower sequency in modifying a transform structure for smooth change.

i	Dyadic Symmetry			Walsh basis vectors $\vec{H}(i)$							
	001	011	111								
0	0	0	0	1	1	1	1	1	1	1	1
1	0	0	1	1	1	1	1	-1	-1	-1	-1
2	0	1	0	1	1	-1	-1	-1	-1	1	1
3	0	1	1	1	1	-1	-1	1	1	-1	-1
4	1	0	0	1	-1	-1	1	1	-1	-1	1
5	1	0	1	1	-1	-1	1	-1	1	1	-1
6	1	1	0	1	-1	1	-1	-1	1	-1	1
7	1	1	1	1	-1	1	-1	1	-1	1	-1

Table 2.2: Sequency-ordered Walsh transform, where under the column of Dyadic Symmetry,

'0' : even dyadic symmetry

'1' : odd dyadic symmetry

Two combinations, namely [T1] and [T2], are examined and expected having better performance. They can be explained as follow :

2.3.2 [T1] = [P] Diag([DM$_2$(4)],[A(4)]) [Q]

Consider $\vec{H}(1)$,

$$\vec{H}(1) : [\ 1\ \ 1\ \ 1\ \ 1\ -1\ -1\ -1\ -1\ ]$$

There is a sudden change between the 3rd and 4th components. If the 1st and 3rd dyadic symmetries in $\vec{H}(1)$ are destroyed, we have a new basis vector :

$$\vec{T1}(1) : [\ a_0\ \ a_1\ \ a_2\ \ a_3\ -a_3\ -a_2\ -a_1\ -a_0\ ]$$

which can have more smooth change if $a_0 \geq a_1 \geq a_2 \geq a_3$. To maintain orthogonality, $\vec{H}(3)$, $\vec{H}(5)$ and $\vec{H}(7)$ also have to be replaced. These four vectors can be self-orthogonal by using Dyadic Matrix, and orthogonal to other four basis vectors (i.e. $\vec{H}(0)$, $\vec{H}(2)$, $\vec{H}(4)$, $\vec{H}(6)$) by

their 7th opposite DS. By examining the structure of $\vec{H}(3)$, it can be expected that replacing [A(4)] by [$DM_2(4)$], defined in section 2.2.1, can generate a better transform matrix. The resulting transform matrix has basis vectors shown in Table 2.3.

i	Dyadic Symmetry			Modified basis vectors $\vec{T1}$(i)							
	001	011	111								
0	0	0	0	1	1	1	1	1	1	1	1
1	x	x	1	a_0	a_1	a_2	a_3	$-a_3$	$-a_2$	$-a_1$	$-a_0$
2	0	1	0	1	1	-1	-1	-1	-1	1	1
3	x	x	1	a_3	a_2	$-a_1$	$-a_0$	a_0	a_1	$-a_2$	$-a_3$
4	1	0	0	1	-1	-1	1	1	-1	-1	1
5	x	x	1	a_2	$-a_3$	$-a_0$	a_1	$-a_1$	a_0	a_3	$-a_2$
6	1	1	0	1	-1	1	-1	-1	1	-1	1
7	x	x	1	a_1	$-a_0$	a_3	$-a_2$	a_2	$-a_3$	a_0	$-a_1$

Table 2.3 : Modified Transform Matrix [T1], where under the column of Dyadic Symmetry,
'0' : even dyadic symmetry
'1' : odd dyadic symmetry
'x' : absence of the dyadic symmetry

Exhaustive search has been used to determine the optimum transform components by varying a_0, a_1, a_2 and a_3 in such a way that a_0, a_1, a_2 and a_3 are all integer, $16 > a_0 \geq a_1 \geq a_2 \geq a_3 > 0$. Under different values of adjacent element correlation ρ, the values of a_0, a_1, a_2 and a_3 that provide the best performance have been found. The results and the corresponding transform performance are shown in Table 2.4.

ρ	a_0	a_1	a_2	a_3	TE	MRB
0.1	7	7	7	5	91.36%	0.00490
0.2	14	14	14	9	84.47%	0.02012
0.3	11	11	10	6	79.58%	0.04720
0.4	13	13	11	6	76.36%	0.08908
0.5	5	5	4	2	74.66%	0.15065
0.6	14	14	11	5	74.32%	0.24022
0.7	10	10	7	3	75.55%	0.37330
0.8	15	15	10	4	78.07%	0.58410
0.9	13	12	8	3	84.94%	0.98196

Table 2.4 : Optimum components and performance of [T1]

2.3.3 [T2] = [P] Diag([$DM_2(4)$],[$DM_2(4)$]) [Q]

In KLT, which is the optimum transform, the 0^{th} basis vector has its magnitude maximum at the centre and decrease in both side to minimum at end components. However, the components of the 0^{th} basis vector in WT, or in the [T1] obtained in last section, have constant value. The vector is commonly referred to as the DC basis vector. For the transform matrix [T1] shown in Table 2.3, there are still four basis vectors remain unchanged and can be modified to resemble that of KLT. If the 1^{st} and 3^{rd} dyadic symmetries in 0^{th} basis vector of [T1] are destroyed, then a new basis vector $\overrightarrow{T2}(0)$ is obtained :

$$\overrightarrow{T2}(0) : [\ b_0\ \ b_1\ \ b_2\ \ b_3\ \ b_3\ \ b_2\ \ b_1\ \ b_0\ ]$$

When $b_0 < b_1 < b_2 < b_3$, $\overrightarrow{T2}(0)$ will resemble the 0^{th} basis vector of KLT. The zeroth-basis-vector-modified transform is expected to have better transform.

To maintain orthogonality, $\overrightarrow{H}(2)$, $\overrightarrow{H}(4)$ and $\overrightarrow{H}(6)$ also have to be replaced. These four basis vectors can be set self-orthogonal by using Dyadic Matrix, and orthogonal to the 1^{st},

3^{rd}, 5^{th} and 7^{th} basis vector by 7^{th} opposite DS. By examining the structure of $\vec{H}(2)$, it can be expected that the use of $DM_2(4)$ can result in a matrix with better transform performance. Table 2.5 shows the resulting matrix obtained in this way :

i	Dyadic Symmetry			Modified basis vectors $\vec{T2}(i)$							
	001	011	111								
0	x	x	0	b_0	b_1	b_2	b_3	b_3	b_2	b_1	b_0
1	x	x	1	a_0	a_1	a_2	a_3	$-a_3$	$-a_2$	$-a_1$	$-a_0$
2	x	x	0	b_3	b_2	$-b_1$	$-b_0$	$-b_0$	$-b_1$	b_2	b_3
3	x	x	1	a_3	a_2	$-a_1$	$-a_0$	a_0	a_1	$-a_2$	$-a_3$
4	x	x	0	b_2	$-b_3$	$-b_0$	b_1	b_1	$-b_0$	$-b_3$	b_2
5	x	x	1	a_2	$-a_3$	$-a_0$	a_1	$-a_1$	a_0	a_3	$-a_2$
6	x	x	0	b_1	$-b_0$	b_3	$-b_2$	$-b_2$	b_3	$-b_0$	b_1
7	x	x	1	a_1	$-a_0$	a_3	$-a_2$	a_2	$-a_3$	a_0	$-a_1$

Table 2.5 : Modified Transform Matrix [T2], where under the column of Dyadic Symmetry,
'0' : even dyadic symmetry
'1' : odd dyadic symmetry
'x' : absence of the dyadic symmetry

By exhaustive search, the optimum sets of (a_0,a_1,a_2,a_3) and (b_0,b_1,b_2,b_3) are found and the performance of the corresponding [T2] are shown in Table 2.6.

ρ	a_0	a_1	a_2	a_3	b_0	b_1	b_2	b_3	TE	MRB
0.1	7	7	7	5	2	5	6	6	93.35%	0.00547
0.2	14	14	14	9	4	9	11	11	87.98%	0.02228
0.3	11	11	10	6	5	11	13	13	83.96%	0.05178
0.4	13	13	11	6	5	10	12	12	81.96%	0.09657
0.5	5	5	4	2	7	12	14	14	81.44%	0.16109
0.6	14	14	11	5	7	11	13	13	81.88%	0.25311
0.7	10	10	7	3	5	7	8	8	84.09%	0.38745
0.8	15	15	10	4	9	11	12	12	88.06%	0.59755
0.9	13	12	8	3	12	13	14	14	92.18%	0.99113

Table 2.6 : Optimum components and performance of [T2]

It is interesting to see that if the values of $(a_0,a_1,a_2,a_3,b_0,b_1,b_2,b_3)$ for different ρ are substituted by the corresponding components in 0^{th} and 1^{st} sequency-ordered basis vectors of KLT, the resulting transform matrix, denoted as MKLT, can also have good performance. The performance of MKLT, KLT and DCT are shown in Table 2.7 below.

	MKLT		KLT		DCT	
ρ	TE	MRB	TE	MRB	TE	MRB
0.1	94.70%	0.00531	100%	0.00634	94.54	0.00583
0.2	90.78%	0.02177	100%	0.02577	90.34	0.02397
0.3	88.14%	0.05085	100%	0.05953	87.12	0.05601
0.4	86.69%	0.09518	100%	0.11005	84.73	0.10464
0.5	86.36%	0.15926	100%	0.18158	83.14	0.17439
0.6	87.11%	0.25095	100%	0.28169	82.44	0.27312
0.7	88.91%	0.38528	100%	0.42500	82.87	0.41584
0.8	91.71%	0.59603	100%	0.64484	84.97	0.63638
0.9	95.45%	0.99070	100%	1.04822	89.83	1.04244

Table 2.7 : Performance of MKLT, KLT and DCT

The basis restriction mean square error for $\rho = 0.9$ have also been computed for [T1], [T2], MKLT, KLT and DCT. They are listed in Table 2.8 for comparison.

v	[T1]	[T2]	MKLT	KLT	KLT
0	1.000	1.000	1.000	1.000	1.000
1	0.227	0.225	0.225	0.225	0.227
2	0.101	0.099	0.099	0.099	0.101
3	0.063	0.062	0.062	0.058	0.058
4	0.047	0.047	0.047	0.037	0.037
5	0.034	0.034	0.034	0.024	0.024
6	0.024	0.023	0.023	0.015	0.015
7	0.011	0.011	0.011	0.007	0.007

Table 2.8 : Basis restriction mean square error for $\rho = 0.9$.

The TE, MRB are shown in Fig.2.1 - Fig.2.2 for comparison.

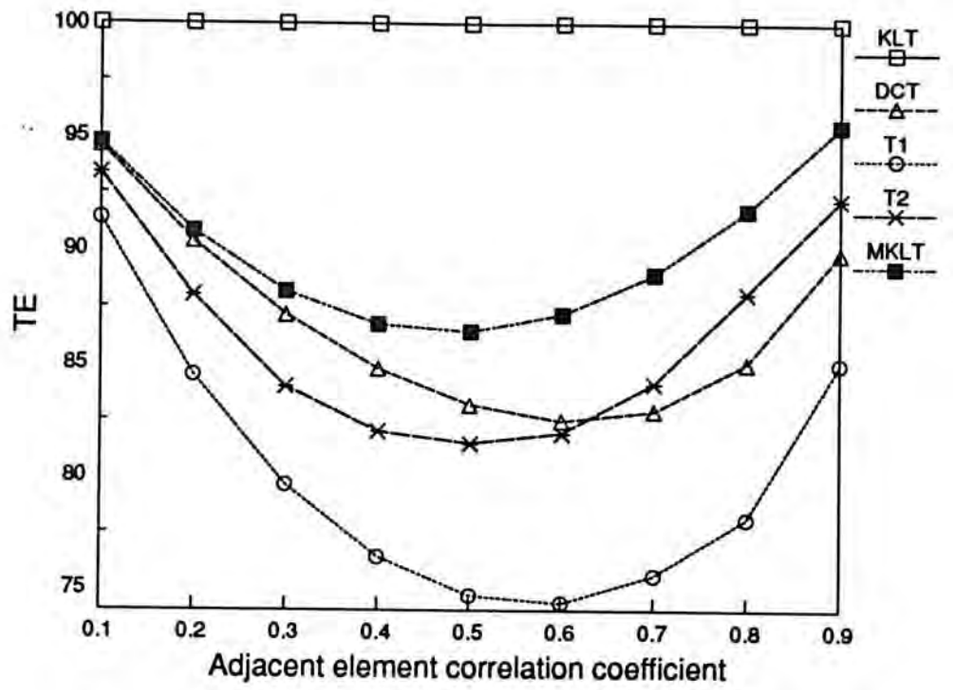

Fig.2.1 Transform efficiency vs adjacent element correlation coefficient

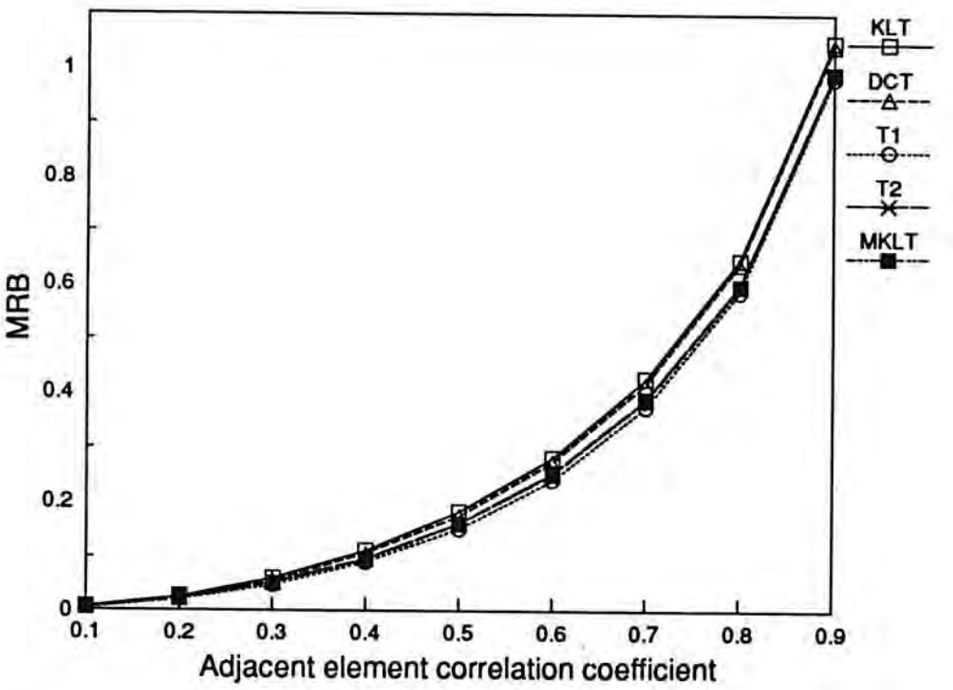

Fig.2.2 Maximum reducible bit vs adjacent element correlation coefficient

2.4 Discussions and Conclusions

In this chapter, the formation of Dyadic Matrices is studied. There are different combinations of dyadic shift which can be used for forming orthogonal Dyadic Matrices [CHAM90]. By examining the conditions of orthogonality of Dyadic Matrix, the sets of dyadic shift obtained in [CHAM90] for forming Dyadic Matrices have been found by a different approach. Moreover, we have proved that the maximum size of Dyadic Matrices is 8.

By using Dyadic Matrix, arbitrary orthogonal matrix can be generated for different application. For example, the use of Dyadic Matrix in destroying dyadic symmetry has been discussed. Two transforms structure, [T1] and [T2] have been proposed by destroying dyadic symmetry and use of Dyadic Matrix. The optimum components of the transform matrices are found by exhaustive search and the transform performance are compared using three performance criteria. In summary, the performance of [T2] is better than [T1]. For adjacent element correlation $\rho > 0.7$, Transform Efficiency shows that [T2] may perform better than DCT and hence can be used as a substitute for DCT.

It is also found that a MKLT can be obtained by using parameters of KLT and the transform structure of [T2]. The performance of MKLT is better than DCT in terms of TE, with only eight variable kernel components. Thus, we can use MKLT in a adaptive transform coding system such that at transmitter, by sending the components of MKLT as overhead, the transform can be adapted to local statistics of an image. At the receiver, the received overhead is used to construct the transform, which then inverse transform the received data to reconstruct the image.

3. LOW SEQUENCY COEFFICIENT TRUNCATION (LSCT) CODING SCHEME

3.1 Introduction

In a traditional transform coding system, monochrome image can be represented by as low as 0.5 bit per pixel (bpp) with reasonable reconstructed image quality [CHENs77]. Usually, DC and AC coefficients are quantized separately. Different schemes have been proposed for quantizing and encoding the AC coefficients [NGAN82] [CLARK85]. However, not much research effort has been put on the encoding of DC coefficients. In most transform coding systems, DC coefficients are encoded by 8 bits. These bits allocated for DC coefficients thus represent a large percentage of bits available for coding, particularly at low bit rate. If these DC coefficients are truncated at the transmitter, those bits originally assigned for DC coefficients can now be allocated to other AC coefficients. Thus, the AC coefficients can be coded more accurately and hence the fine detail of the image could be better maintained. At the receiver, the DC coefficients can be estimated to reconstruct the image. This DC coefficient truncation and restoration scheme has been reported in [CHAMc84] and it was used together with the C&S system [CHENs77] but only marginal improvement in performance was achieved [YIP88].

A DC coefficient restoration scheme can be viewed as a low sequency coefficient restoration scheme [CHAMc84]. The low sequency Walsh transform coefficients for a block of data, after a transformation, correspond to DC coefficients of low order subblock in the data set. For example, consider a set of data with 16 elements $[x_0,x_1,...,x_{15}]$. Divide the set of data into four subblocks, $[x_0,...,x_3]$, $[x_4,...,x_7]$, $[x_8,...,x_{11}]$ and $[x_{12},...,x_{15}]$, and let the DC coefficients of these four subblock be d_0,d_1,d_2 and d_3 respectively. Then it has been found that the first four low sequency Walsh coefficients $[c_0,c_1,c_2,c_3]$ of $[x_0,x_1,...,x_{15}]$ correspond to $[d_0,d_1,d_2,d_3]$. If $[c_0,c_1,c_2,c_3]$ of the Walsh transform coefficients are truncated, the effect is simply like truncating

the DC coefficients $[d_0,d_1,d_2,d_3]$. Thus, truncating low sequency coefficients is equivalent to truncating the DC coefficients, or resetting the mean, of each subblock to zero. The original data set $[x_0,x_1,...,x_{15}]$ can be restored by estimating the DC coefficients of each subblock.

Hence, we can extend the DC coefficients truncation and restoration scheme to a Low Sequency Coefficient Truncation (LSCT) scheme. In our LSCT scheme, not only the DC coefficients, but also some low sequency coefficients are truncated. As a result, the bits originally assigned for those transform coefficients truncated can now be used to encode other AC coefficients more accurately and we expect that the visual quality of the image should be better as AC information is more accurately encoded. At the receiver, we can obtain the reconstructed image by estimating the DC coefficients of each subblock, using the methods in [CHAMc84].

In the following sections, three DC coefficient estimation techniques [CHAMc84] will be described. All three techniques have been used in the LSCT schemes. In section 3.3, Low Sequency Coefficient Truncation (LSCT) scheme 1 will be described and simulation results are given. By looking at the defect of LSCT scheme 1, another LSCT scheme 2 will be described in section 3.4 for better performance. Simulation results are also given for comparison. Conclusion will then be drawn in section 3.5.

3.2 DC Coefficient Estimation Schemes

3.2.1 Element Estimation

In this method, a DC coefficient of $(k,l)^{th}$ block is estimated from its vertical and horizontal adjacent blocks, as shown in Fig 3.1.

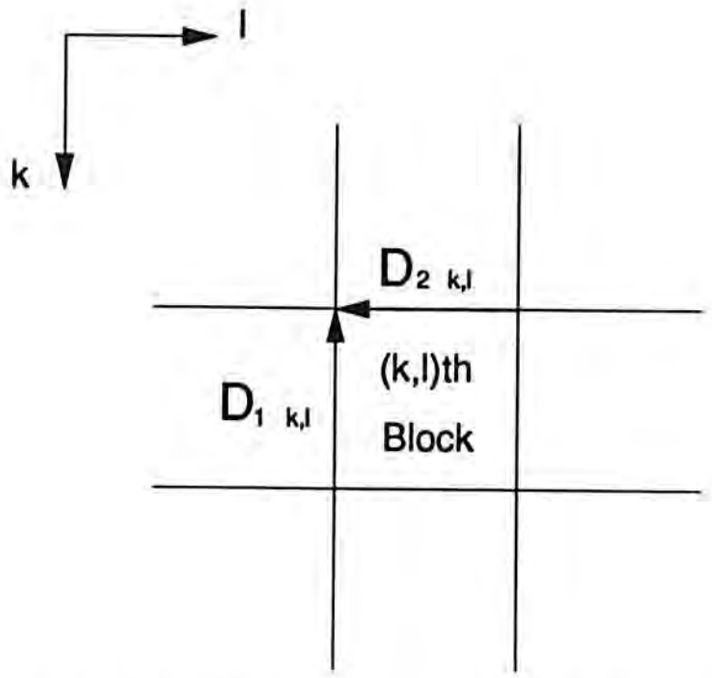

Fig.3.1 The two edge difference vectors considered in element estimation

Let a_{kl} represent the DC coefficient of $(k,l)^{th}$ block and $u_{kl}(p,q)$ represent the $(p,q)^{th}$ zero DC pixel element of the $(k,l)^{th}$ block. The vertical edge difference vector, $D_{1\,k,l}$, and horizontal edge difference vector, $D_{2\,k,l}$, are defined as :

$$D_{1\,k,l} = a_{k,l-1} \times V + \begin{bmatrix} u_{k,l-1}(0,N-1) - u_{k,l}(0,0) \\ u_{k,l-1}(1,N-1) - u_{k,l}(1,0) \\ u_{k,l-1}(2,N-1) - u_{k,l}(2,0) \\ \vdots \\ u_{k,l-1}(N-1,N-1) - u_{k,l}(N-1,0) \end{bmatrix} \tag{3.1a}$$

$$D_{2\,k,l} = a_{k-1,l} \times V + \begin{bmatrix} u_{k-1,l}(N-1,0) - u_{k,l}(0,0) \\ u_{k-1,l}(N-1,1) - u_{k,l}(0,1) \\ u_{k-1,l}(N-1,2) - u_{k,l}(0,2) \\ \vdots \\ u_{k-1,l}(N-1,N-1) - u_{k,l}(0,N-1) \end{bmatrix} \tag{3.1b}$$

where k,l ∈ [1,M-1], M is the number of blocks in a row and V is a vector at the edge of the NxN DC basis picture, i.e.

$$V=\left[\frac{1}{N}\ \frac{1}{N}\ \cdots\ \frac{1}{N}\right]^t \tag{3.2}$$

If a DC coefficient, a_{kl}, is added to the $(k,l)^{th}$ block, then the two edge difference vectors are changed to a new vertical edge difference vector $W_{1k,l}$ and a new horizontal edge difference vector $W_{2k,l}$:

$$W_{1\,k,l}=D_{1\,k,l}-a_{k,l}\times V \tag{3.3a}$$

$$W_{2\,k,l}=D_{2\,k,l}-a_{k,l}\times V \tag{3.3b}$$

The estimated DC coefficient of the current $(k,l)^{th}$ block is the one which minimizes the mean square edge difference, e, between the current block and adjacent blocks, i.e.

$$e=|W_{1\,k,l}|^2+|W_{2\,k,l}|^2 \tag{3.4}$$

It can be shown that the estimated DC coefficient is :

$$a_{k,l}=\frac{1}{2}\times\sum_{p=1}^{2}\sum_{m=0}^{N-1}d(p,m)_{k,l} \tag{3.5}$$

where $d(p,m)_{k,l}$ is the m^{th} element of the vector $D_{p\,k,l}$.

3.2.2 Row Estimation

The second method of DC coefficient estimation is by determining the set of DC coefficients of a row simultaneously, as shown in Fig.3.2.

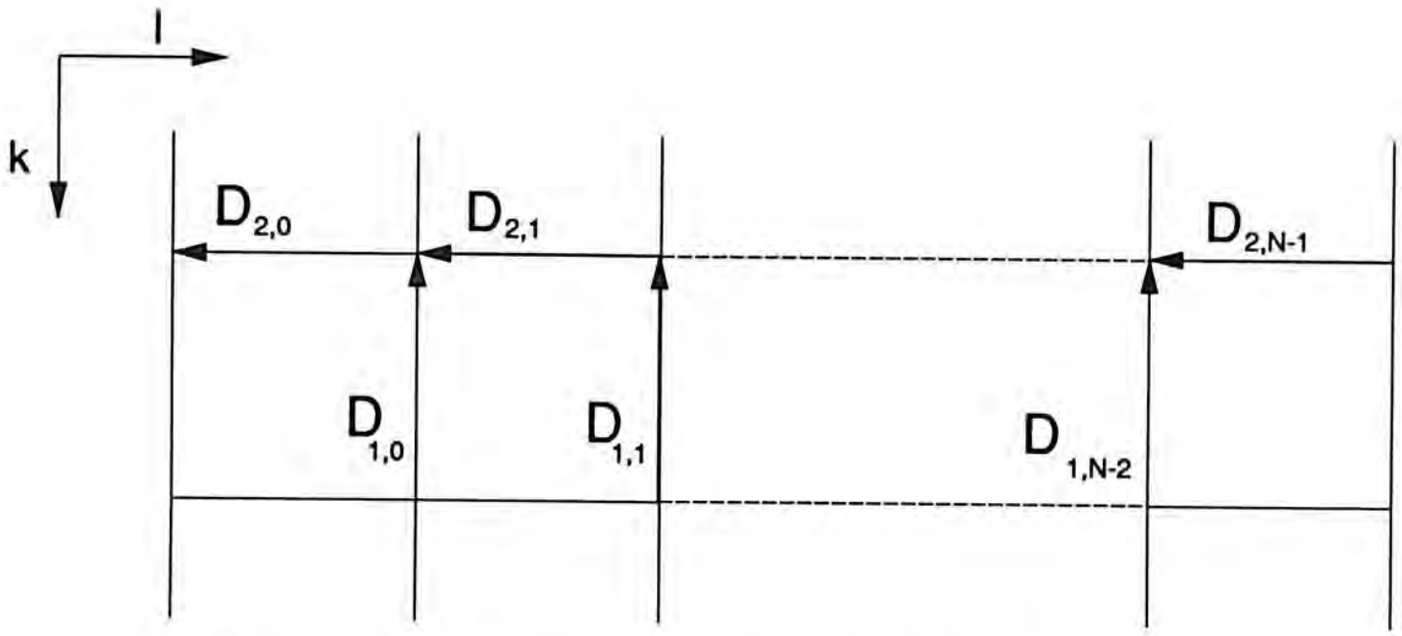

Fig.3.2 The edge difference vectors considered in row estimation

Let $v_{k-1,l}(p,q)$ be the $(p,q)^{th}$ pel in $(k-1,l)^{th}$ block, in which the DC level has been adjusted according to the previously estimated DC coefficients.

A N-dimensional DC coefficient vector $\vec{A}$ is defined whose components are the DC coefficients of the current row :

$$\vec{A} = [a_0, a_1, ..., a_{N-1}] \tag{3.6}$$

As shown in Fig.3.2, the vertical edge vector, $D_{1\,l}$, between the l^{th} block and $(l+1)^{th}$ block in k^{th} row is defined as :

$$D_{1\,l} = \begin{bmatrix} u_{k,l}(0,N-1) & - & u_{k,l+1}(0,0) \\ u_{k,l}(1,N-1) & - & u_{k,l+1}(1,0) \\ u_{k,l}(2,N-1) & - & u_{k,l+1}(2,0) \\ \vdots & & \\ u_{k,l}(N-1,N-1) & - & u_{k,l+1}(N-1,0) \end{bmatrix} \quad l \in [0,N-2] \tag{3.7a}$$

The horizontal edge vector, $D_{2\,l}$, between the $(k\text{-}1,l)^{th}$ block and $(k,l)^{th}$ block is defined as :

$$D_{2l}=\begin{bmatrix} u_{k,l}(N\text{-}1,0) - v_{k\text{-}1,l}(0,0) \\ u_{k,l}(N\text{-}1,1) - v_{k\text{-}1,l}(0,1) \\ u_{k,l}(N\text{-}1,2) - v_{k\text{-}1,l}(0,2) \\ \vdots \\ u_{k,l}(N\text{-}1,N\text{-}1) - v_{k\text{-}1,l}(0,N\text{-}1) \end{bmatrix} \quad l \in [0,N\text{-}1] \tag{3.7b}$$

If the estimated DC coefficients are added to corresponding blocks in k^{th} row, the edge difference vectors $D_{1\,l}$ and $D_{2\,l}$ are changed to $W_{1\,l}$ and $W_{2\,l}$ respectively :

$$W_{1l}=D_{1l}+(a_l-a_{l+1})\times V \tag{3.8a}$$

$$W_{2l}=D_{2l}+a_l\times V \tag{3.8b}$$

By minimizing the sum of the square of the magnitudes of these edge difference vectors :

$$e=\sum_{l=0}^{N-2}|W_{1l}|^2+\sum_{l=0}^{N-1}|W_{2l}|^2 \tag{3.9}$$

It has been shown that the estimated DC coefficients, or $\vec{A}$, is given by :

$$\vec{A}=-[RR]^{-1}\times C \tag{3.10}$$

where

$$[RR] = \frac{1}{N} \times \begin{bmatrix} 2 & -1 & 0 & . & . & . & . & . & . \\ -1 & 3 & -1 & 0 & . & . & . & . & . \\ 0 & -1 & 3 & -1 & 0 & . & . & . & . \\ . & 0 & -1 & 3 & -1 & 0 & . & . & . \\ . & . & . & . & . & . & . & . & . \\ . & . & . & . & . & . & . & . & . \\ . & . & . & . & 0 & -1 & 3 & -1 & 0 \\ . & . & . & . & . & 0 & -1 & 3 & -1 \\ . & . & . & . & . & . & 0 & -1 & 2 \end{bmatrix} \tag{3.11}$$

$$C = \sum_{j=1}^{2} \sum_{k=0}^{N-1} [R]_{j,k}^{t} \times D_{j,k} \tag{3.12}$$

$$[R]_{11}(p,q) = \begin{cases} 0 & , \quad \text{if } l = M-1 \\ \frac{1}{N} & , \quad \text{if } l \neq M-1,\ q = l \\ -\frac{1}{N} & , \quad \text{if } l \neq M-1,\ q = l+1 \\ 0 & , \quad \text{if } l \neq M-1,\ q \neq l,\ q \neq l+1 \end{cases} \tag{3,13a}$$

$$[R]_{21}(p,q) = \begin{cases} \frac{1}{N} & , \quad \text{if } q = 1 \\ 0 & , \quad \text{if } q \neq 1 \end{cases} \tag{3,13b}$$

3.2.3 Plane Estimation

In this method, the DC coefficients of four adjacent blocks, as shown in Fig.3.3, are estimated using the four edge difference vectors D_1, D_2, D_3, D_4.

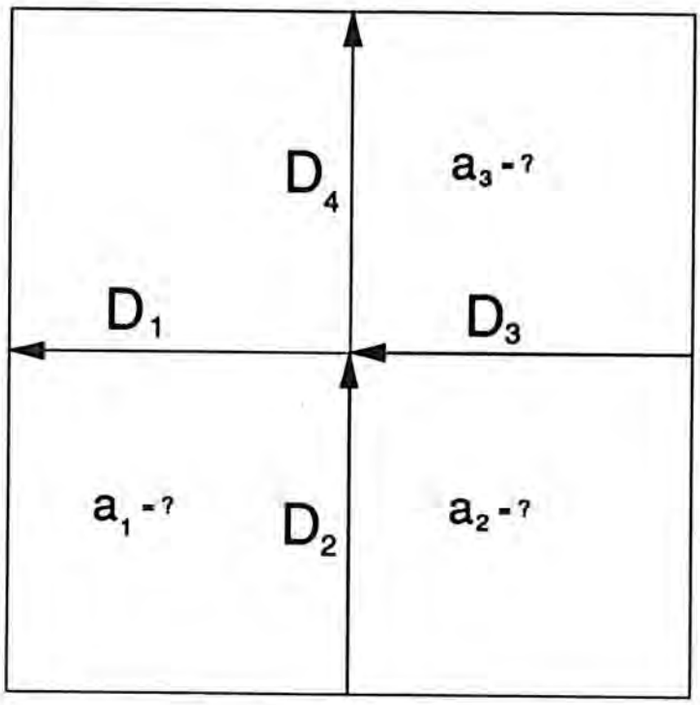

Fig.3.3 The edge difference vectors considered in plane estimation

The four edge difference vectors are defined as :

$$D_1 = \begin{bmatrix} u_{0,0}(N\text{-}1,0) - u_{1,0}(0,0) \\ u_{0,0}(N\text{-}1,1) - u_{1,0}(0,1) \\ \vdots \\ u_{0,0}(N\text{-}1,N\text{-}1) - u_{1,0}(0,N\text{-}1) \end{bmatrix} \tag{3.14a}$$

$$D_2 = \begin{bmatrix} u_{1,0}(0,N\text{-}1) - u_{1,1}(0,0) \\ u_{1,0}(1,N\text{-}1) - u_{1,1}(1,0) \\ \vdots \\ u_{1,0}(N\text{-}1,N\text{-}1) - u_{1,1}(N\text{-}1,0) \end{bmatrix} \tag{3.14b}$$

$$D_3 = \begin{bmatrix} u_{0,1}(N\text{-}1,0) - u_{1,1}(0,0) \\ u_{0,1}(N\text{-}1,1) - u_{1,1}(0,1) \\ \cdot \\ \cdot \\ \cdot \\ u_{0,1}(N\text{-}1,N\text{-}1) - u_{1,1}(0,N\text{-}1) \end{bmatrix} \tag{3.14c}$$

$$D_4 = \begin{bmatrix} u_{0,0}(0,N\text{-}1) - u_{0,1}(0,0) \\ u_{0,0}(1,N\text{-}1) - u_{1,0}(0,1) \\ \cdot \\ \cdot \\ \cdot \\ u_{0,0}(N\text{-}1,N\text{-}1) - u_{0,1}(N\text{-}1,0) \end{bmatrix} \tag{3.14d}$$

After adjusting the pels in $(1,0)^{th}$, $(1,1)^{th}$ and $(0,1)^{th}$ blocks in accordance with the estimated a_{10},a_{11} and a_{01}, we have the following new edge difference vectors :

$$W_1 = D_1 - V \cdot a_{10} \tag{3.15a}$$

$$W_2 = D_2 + V \cdot (a_{10} - a_{11}) \tag{3.15b}$$

$$W_3 = D_3 + V \cdot (a_{01} - a_{11}) \tag{3.15c}$$

$$W_4 = D_4 - V \cdot a_{01} \tag{3.15d}$$

Let

$$A = [a_{10}, a_{11}, a_{01}]^t.$$

$$[R_1] = [-V,0,0]$$

$$[R_2] = [V,-V,0]$$

$$[R_3] = [0,-V,V]$$

$$[R_4] = [0,0,-V]$$

The sum of the squares of the four new edge difference vector magnitudes can be expressed as :

$$e = \sum_{p=1}^{4} | D_p + [R_p] \times A |^2 \tag{3.16}$$

By minimizing eq.(3.16) with respect to a_{10}, a_{11}, a_{01}, we can obtain the estimated DC coefficients. Let $d(i)_p$ be the i^{th} element of vector D_p and $s(p)$ be the average of elements in vector D_p, i.e.

$$D_p = \begin{bmatrix} d(0)_p \\ d(1)_p \\ \cdot \\ \cdot \\ \cdot \\ d(N-1)_p \end{bmatrix} \tag{3.17}$$

$$s(p) = \frac{1}{N} \times \sum_{i=0}^{N-1} d(i)_p \tag{3.18}$$

The estimated DC coefficients are given by

$$a_{10} = [s(4) + s(3) - s(2) + 3s(1)] / 4 \tag{3.19a}$$

$$a_{11} = [s(4) + s(3) + s(2) + s(1)] / 2 \tag{3.19b}$$

$$a_{01} = [3s(4) - s(3) + s(2) + s(1)] / 4 \tag{3.19c}$$

In next section, these three schemes will be used in estimating the DC coefficients.

3.3 LSCT Coding Scheme 1 and Results

In this scheme, the coding system is basically the same as the C&S system [CHENs77]. However, according to the class of each block, some low sequency coefficients of that block will be truncated. The details of which are described as follow :

In the transmitter, an image is divided into 8x8 blocks and transformed. The AC energy of each block is calculated. According to AC energy calculated, each block is classified into one of the four classes in the same way as the C&S system. The classification of blocks is such that the number of blocks in each class is the same. A class map is then generated as an overhead, indicating the class of each block. In our LSCT scheme 1, low sequency coefficients in each class are truncated as follow :

class 0 : DC coefficient is truncated.

class 1 : DC coefficient is truncated.

class 2 : 2x2 lowest sequency coefficients are truncated.

class 3 : 4x4 lowest sequency coefficients are truncated.

Afterwards, the bit allocation, quantization and coefficient encoding are similar to those of C&S system. As the information of the number of low sequency coefficient truncated is included in the class map, no additional overhead is required with respect to the C&S system.

In the receiver, the transform coefficients are inverse transformed to spatial domain. As mentioned, truncating low sequency coefficients is equivalent to truncating DC coefficients of lower order subblocks. Thus we now have to estimate the DC coefficients of subblocks for class 2 and class 3. For class 3, 4x4 low sequency coefficients have been truncated. Thus, the following procedures are used to reconstruct the image block :

1. The 8x8 blocks in spatial domain are divided into sixteen 2x2 blocks. Every four adjacent blocks have their DC coefficients estimated using Plane Estimation. Then each 2x2 block is adjusted by its corresponding DC coefficient.

2. The 8x8 blocks are now divided into four 4x4 blocks. The DC coefficients of these 4x4 blocks are again estimated using Plane Estimation and added to corresponding blocks.

For class 2, as 2x2 transform coefficients are truncated, only the procedure 2 described above is needed.

Now all blocks should have their DC coefficients of each subblock estimated. The final step is to estimate the DC coefficients for each block in a row. The method used is the Row Estimation because it gives the best performance as reported in [CHAMc84].

Now we compare the performance of LSCT scheme 1 with that of C&S. Before that, performance criterion has to be defined first. In the simulation described throughout the thesis, the Mean Square Error (MSE) will be used as the criterion for coding systems performance evaluation. The MSE is defined as :

$$\mathrm{MSE} = \frac{1}{256\mathrm{x}256} \sum_{i,j=0}^{255} [f(i,j) - \hat{f}(i,j)]^2 \qquad (3.20)$$

where $f(i,j)$: $(i,j)^{th}$ pixel of original image

$\hat{f}(i,j)$: $(i,j)^{th}$ pixel of reconstructed image

Table 3.4 and 3.5 shows the MSE performance for the C&S scheme and LSCT scheme 1 respectively. To assess the visual quality of reconstructed images, images LENNA and BABOON will be used throughout the thesis for comparison. Their original images are shown in Fig.3.4. The reconstructed images, LENNA and BABOON, after being processed by C&S system and LSCT scheme 1 are also shown in Fig.3.5 and Fig.3.6 respectively. As expected,

the MSE performance of LSCT scheme 1 is poor when compared with the C&S scheme. We expect that the LSCT scheme would produce images with better visual quality than the C&S scheme because the AC coefficients of the LSCT scheme are coded more accurately. However, the visual quality of the reconstructed images is also not acceptable. The poor performance of LSCT scheme 1 may be due to the following reasons :

1. There is a large estimation error between the original and estimated DC coefficients.

2. For class 2 and class 3, not only the DC coefficients but also more low sequency coefficients are truncated. As the estimation of DC coefficients depends on information provided by high sequency coefficients, more coefficient truncation means less high sequency coefficients or information can be used for estimation. Thus, the estimated DC coefficients have large error.

3. We expect that the high sequency coefficients, when transformed back to spatial domain, can be used for low sequency coefficient estimation. This is true when there is no quantization. But in practical system, the high sequency coefficients are quantized. Because of the quantization error, the estimation of DC coefficients based on these quantized coefficients is erroneous.

4. The estimation of DC coefficients by Row Estimation uses information from previous row. However, there is already large estimation error in the previous row and the error in previous row will hence propagate to the current row. As a result, the estimation error is again enlarged.

In summary, due to the reasons given above, the LSCT scheme 1 cannot give satisfactory performance as expected.

	LENNA			PEPPERS			SAILBOAT			BABOON		
Bit rate	1.00	0.75	0.50	1.00	0.75	0.50	1.00	0.75	0.50	1.00	0.75	0.50
MSE	49.4	72.9	106.0	52.3	75.1	114.2	118.6	168.4	241.5	284.7	375.0	488.3

Table 3.1 Simulation result for C&S scheme.

	LENNA			PEPPERS			SAILBOAT			BABOON		
Bit rate	1.00	0.75	0.50	1.00	0.75	0.50	1.00	0.75	0.50	1.00	0.75	0.50
MSE	231.4	292.2	461.7	441.7	635.6	675.5	904.0	1040.0	1263.7	1211.9	1212.6	1538.5

Table 3.2 Simulation result for LSCT scheme 1.

(a) LENNA (b) BABOON

Fig.3.4 Original images

(a) LENNA, 0.5 bpp

(d) BABOON, 0.5 bpp

(b) LENNA, 0.75 bpp

(e) BABOON, 0.75 bpp

(c) LENNA, 1.0 bpp

(f) BABOON, 1.0 bpp

Fig.3.5 Images after processed by C&S scheme

(a) LENNA, 0.5 bpp

(d) BABOON, 0.5 bpp

(b) LENNA, 0.75 bpp

(e) BABOON, 0.75 bpp

(c) LENNA, 1.0 bpp

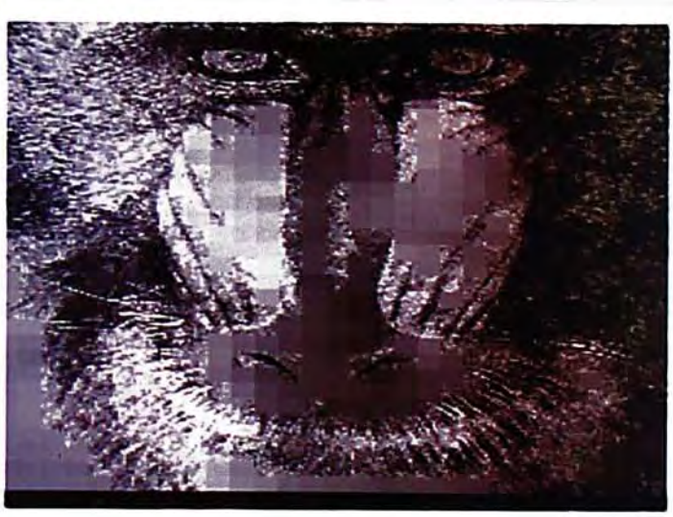

(f) BABOON, 1.0 bpp

Fig.3.6 Images after processed by LSCT scheme 1

3.4 LSCT Coding Scheme 2 and Results

In LSCT scheme 2, we try to improve the coding method of LSCT scheme 1 such that better performance in both MSE and visual quality can be obtained. As discussed in LSCT scheme 1, the large number of coefficients truncated causes unsatisfactory result. So we try to limit the maximum number of coefficients to be truncated to only 2x2, even for class 2 and class 3. Thus, there will not have too much coefficient truncation and hence the estimation of DC coefficients will be more accurate.

Moreover, the propagation of estimation error should be avoided such that the previous estimation error would not result in current estimation a larger error. In LSCT scheme 2, the Plane Estimation used in LSCT scheme 1 is still employed to estimate DC coefficient of each subblock. Then the Element Estimation is used to estimate the DC coefficients block by block. The resulting errors between original and estimated DC coefficients of each subblock are quantized, using a quantizer developed in [BRAINp90].[1] The quantized errors are then sent to receiver for reconstruction. Thus, the DC coefficients are estimated block by block and the errors are immediately adjusted instead of propagating over the entire image.

Two variations of scheme 2, S2.1 and S2.2, were simulated. In scheme S2.1, the blocks of class 2 and class 3 will have their 2x2 low sequency coefficients truncated. Class 0 and class 1 will have their DC coefficients truncated only. Different number of bits B_e are used to send the error between original and estimated DC coefficients and the simulation results are

---

1 In [BRAINp90], predictors are designed for several test picture and quantizers are designed, using the MSE criterion, for quantizing the error between original and predicted luminance signal. The parameters of the quantizers have been designed based on statistics from several test pictures, with an assumption that the error is Laplacian distributed.

shown in Table 3.3. In scheme S2.2, the blocks of class 2 will have their 2x2 low sequency coefficients truncated. Class 0, class 1 and also class 3 will have DC coefficients truncated only. Different number of bits are also used and the simulation results are shown in Table 3.4.

	LENNA			PEPPERS			SAILBOAT			BABOON		
Bit rate	1.00	0.75	0.50	1.00	0.75	0.50	1.00	0.75	0.50	1.00	0.75	0.50
$B_c = 3$	59.8	82.8	114.8	66.2	88.1	124.0	140.8	192.7	264.0	311.7	389.8	509.6
$B_c = 4$	57.0	81.4	117.8	63.1	84.9	128.5	140.8	185.0	273.1	316.3	402.6	510.0

Table 3.3 Simulation result for LSCT scheme S2.1.

	LENNA			PEPPERS			SAILBOAT			BABOON		
Bit rate	1.00	0.75	0.50	1.00	0.75	0.50	1.00	0.75	0.50	1.00	0.75	0.50
$B_c = 3$	54.9	79.3	107.0	62.7	80.8	118.5	137.3	177.6	243.5	301.9	380.7	488.4
$B_c = 4$	53.3	77.3	106.8	59.6	80.6	117.5	131.9	179.8	248.2	301.2	381.2	495.5

Table 3.4 Simulation result for LSCT scheme S2.2.

It can be seen that both the scheme S2.1 and S2.2 of LSCT scheme 2 give a much lower MSE over that of LSCT scheme 1 and is comparable to C&S system. Images LENNA and PEPPERS have lower MSE when 4-bit quantizer is used. However, images SAILBOAT and BABOON have lower MSE when 3-bit quantizer is used. This is due to the fact that SAILBOAT and BABOON have larger activity and more energy is distributed over the high sequency coefficients. When 4-bit quantizer is used, less bits can be allocated to the high sequency coefficients, which are thus coded less accurately. Thus, the resulting MSE is larger.

Comparing the two schemes, S2.1 and S2.2, with different number of low sequency coefficients truncated for each class, it can be seen that the second one gives a better result. The reason is that for class 3, the activity is too low and most information is contained in low sequency coefficients. Truncating 2x2 coefficients for class 3 is still too much for the estimation to be accurate, which thus results in a larger MSE. Thus scheme S2.2 is better than scheme S2.1. In Fig.3.7, images of LENNA and BABOON after being processed by subscheme S2.2 are shown. It can be seen that the visual quality of images with S2.2 is much better than LSCT scheme 1 and is comparable to C&S system.

In summary, LSCT scheme 2 can give improvement and correct the defect in LSCT scheme 1. However, as bits are required to code the error, less bit can be used to code the high sequency coefficients and hence LSCT scheme 2 still cannot perform better than the C&S system. We expect that if the error can be sent more effectively, then the performance of such LSCT scheme can be better.

(a) LENNA, 0.5 bpp

(d) BABOON, 0.5 bpp

(b) LENNA, 0.75 bpp

(e) BABOON, 0.75 bpp

(c) LENNA, 1.0 bpp

(f) BABOON, 1.0 bpp

Fig.3.7 Images after processed by LSCT scheme S2.2

3.5 Discussions and Conclusions

DC coefficients truncation and restoration have been studied and reported in [CHAMc84] and [YIP88]. Their results have shown that by truncating the DC coefficients, more bits can be allocated for AC coefficients. Performance improvement has been obtained in [YIP88] as the AC coefficients are coded more accurately. In this chapter, the investigation of truncating not only DC coefficients but also low sequency coefficients has been presented. By truncating low sequency coefficients, more bits can be assigned for AC coefficients and hence better performance was expected. The C&S scheme is used as a basis for comparison, in which we truncate more low sequency coefficients as the activity of the block decreases. In LSCT scheme 1, the number of coefficients truncated is determined by the class map in C&S scheme and so no additional overhead is required. However, due to the truncation error, quantization error and error propagation, the estimation of low sequency coefficients is not accurate enough and the results are not satisfactory.

A second scheme, LSCT scheme 2, is then proposed in which the error of estimation is sent to receiver such that the DC coefficients can be adjusted immediately for each block. Moreover, the number of coefficients to be truncated is lower, even for blocks with lower activity. The results, although show much improvement over those of LSCT 1, still cannot perform better than the C&S scheme. The major reason is that larger number of bits is required to send the error. It can be expected that by using more effective quantizer and encoder for the error, better results can be obtained.

In conclusion, low sequency coefficient truncation and estimation can conceptually be used to save more bits and code AC coefficients more accurately. However, quantization and truncation of coefficients in practical transform coding system degrades the accuracy of the DC coefficient estimation. So the reconstructed images do not have much improved quality.

4. VARIABLE BLOCK SIZE (VBS) CODING SCHEME

4.1 Introduction

As real images often have inhomogeneous statistics over different areas, adaptivity has to be incorporated into a transform coding system according to the local activity for the greatest benefit. Usually, there are several parameters in a transform coding system which can be made adaptive to an image. For example, quantizer step size [JAIN81] [NGAN82], bit allocation [CHENs77], transform kernel [TASTOw71] [CHAMac84], and block size used to partition an image [VAISEg87] [CHEN89] can be adaptive. In this chapter, the technique of variable block size (VBS) will be studied for improving the performance of a transform coding system.

In most existing transform coding systems, the block size used to divide an input image is fixed. The commonly used block sizes are 8x8 or 16x16. This approach, however, has not taken into consideration that image statistics may be inhomogeneous and vary from area to area in an image. Some areas of an image may have only smooth changes and contain no high contrast edge. In these areas, higher compression can be obtained by using a larger block size. For those areas containing high activities and contrast edges, a transform of a smaller block size should be used to obtain better local adaptivity and visual quality. Therefore, to truly adapt to the local statistics of an image in different areas, a transform coding system should vary the block size to yield a better trade off between the bit rate and the quality of decoded images.

In [VAISEg87], the variable block size technique has been used to encode images. His system first divides an image into blocks. The local mean of each block is calculated and if it is larger than a threshold, it is subtracted from the block. Then each block will be partitioned into smaller subblocks and undergoes the same mean-removal and

block-partitioning processes until the smallest block size is reached. After the mean-removal process is completed, the variances of the residual, or mean-removed, image blocks are calculated. A hybrid transform coding and vector quantization scheme is then applied to each block, with suitable block size indicated by the variance. Although it was said that satisfactory results can be obtained, the system employs several procedures and coding methods, which complicates its implementation.

Another VBS coding system is proposed in [CHEN89]. His VBS system uses transform coding techniques and has shown performance improvement over fixed block size transform coding system. This VBS transform coding system is much simpler than that in [VAISEg87] and uses a mean-difference based criterion to determine whether a block contains high contrast edges or not. If a block contains high contrast edges, the block is divided into four smaller blocks and the process repeats with the divided blocks until the four blocks contain no further high contrast edges or the smallest block size is reached. After determining the block size for different areas in an image, DCT is applied and the transform coefficients are quantized and encoded similarly as [CHENp84].

Comparing the system in [VAISEg87] and [CHEN89], we can see that Chen's system has a simpler configuration and uses the transform coding technique. So in this chapter, Chen's system will be used as a basis for study. Moreover, we propose a new criterion function, namely Edge Discriminator (ED), to determine whether a block should be divided into smaller ones. By using the ED criterion, the performance of Chen's VBS coding system can be improved.

In the following section, the details of Chen's coding scheme will be briefly described. The proposed Edge Discriminator (ED) will be defined in section 4.3. Simulation results given in section 4.4 show that the proposed criterion function gives better performance improvement over that of Chen's system. Finally, conclusion will be drawn in section 4.5.

4.2 Chen's VBS coding scheme and its limitation

In Chen's variable block size coding system [CHEN89], an image is first divided into 16x16 blocks. In each of these blocks, it is further divided into four 8x8 quadrants.

A decision criterion is then applied to see if each quadrant should be encoded as four independent 4x4 subblocks or as a one 8x8 block. If all of these four quadrants can be encoded as 8x8 blocks, the criterion is again applied to see if the four 8x8 blocks can be further merged and encoded as one 16x16 block. Thus, blocks with high local activities will be encoded as 4x4 blocks and those with low local activities will be encoded as 16x16 blocks. Blocks with size 8x8 are used for those areas with medium activity. The maximum and minimum sizes of encoded blocks are 16x16 and 4x4 respectively. Ideally, if the decision criterion can make appropriate decision at boundaries where there are changes in the image statistics, the divided blocks should have only low activity or uniform change within them. After determining the block size, each block is transformed by DCT of corresponding size. Quantization and coefficient coding are then applied to obtain the encoded data.

To reconstruct the original image, the decoding algorithm has to know the block sizes used in different parts of an image. In [CHEN89], a hierarchical data structure, quadtree, is used. An example of a K-level quadtree structure is shown in Fig.4.1. A quadtree is said to be a K-level quadtree if the lowest level allowed is K-1. When using a K-level quadtree to represent the variable block size scheme, the l^{th} level nodes represent the blocks with size NxN, where $N = N_{min} x 2^{[(K-1)-l]}$, N_{min} is the minimum block size and $l \in [0,K-1]$. The quadtree can be represented by assigning 0 to non-leaf nodes and 1 to leaf nodes. Each node in a quadtree represents a block. If a block can be split into four quadrants, then the corresponding node will generate four children nodes. Otherwise the node becomes a leaf.

In the variable block size transform coding system described, there are three levels in the quadtree. The highest level or the root, represents the 16x16 block and the leaves at lowest level represent 4x4 blocks.

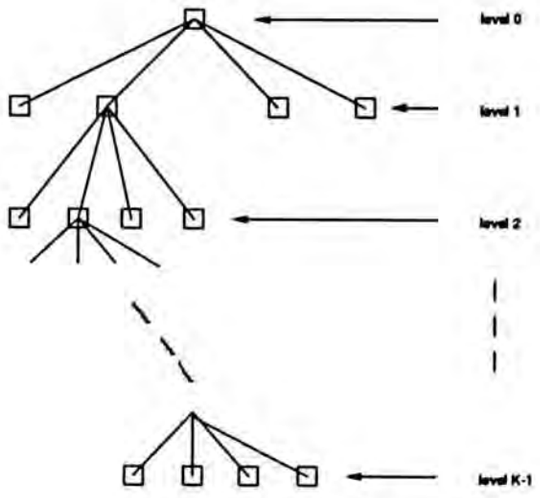

Fig.4.1 An example of K-level quadtree.

In the VBS coding system, a full K-level quadtree is initialized before the process of determining block size starts. All leaves are assigned 1 and the remaining nodes are assigned 0. For every four leaves belonging to the same parent, the decision criterion is applied to see if the blocks represented by them can be merged. If 'yes', these four leaves will be removed and their parent becomes a leaf and is represented by 1. Otherwise, the four leaves remain unchanged. The test-and-merge process repeats with other groups of leaves until the root is reached. After the final quadtree is obtained, the DCT is applied to blocks corresponding to each leaves. The size is determined by the level in which the leaf lies. Transform coefficients can be quantized and coded by using a standard coding scheme [CHENp84]. The quadtree structure is sent as an overhead to the receiver for image reconstruction.

One of the factors that contributes to a successful variable block size coding scheme is the decision criterion. A good decision criterion should be able to determine whether four adjacent NxN blocks should be merged and encoded as a 2Nx2N block. Ideally, if 2Nx2N blocks contain only smooth changes and no high contrast edge, the blocks should be merged and encoded as a 2Nx2N block. Otherwise, the blocks should be divided into four NxN blocks, each of which should have lower activity and hence can be encoded better.

In Chen's system [CHEN89], the decision is based on a Mean Difference Discriminator (MDD) of four adjacent blocks. Four NxN blocks are to be tested if they can be merged into one 2Nx2N block. Let b_{kl} be the mean of $(k,l)^{th}$ block, $i,j,k,l \in [0,1]$, as shown in Fig.4.2. The Chen's MDD criterion can be stated as :

If $|b_{i,j} - b_{k,l}| < t$ for all $(i,j) \neq (k,l)$, then merge

else do not merge.

where t is a decision threshold which can be set empirically.

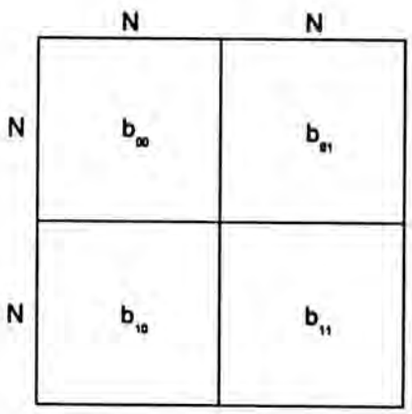

Fig.4.2 The four NxN blocks under consideration

This criterion is simple. However, it is not a good criterion as the mean difference does not necessarily indicate whether the block contains high contrast edges. Hence we propose a new decision criterion, namely the Edge Discriminator (ED), as described in the following section.

4.3 VBS coding scheme with block size determined using Edge Discriminator (ED)

The plane estimator for estimating DC coefficients in [CHAMc84] is used as the Edge Discriminator (ED). Consider four adjacent blocks as shown in Fig.4.3.

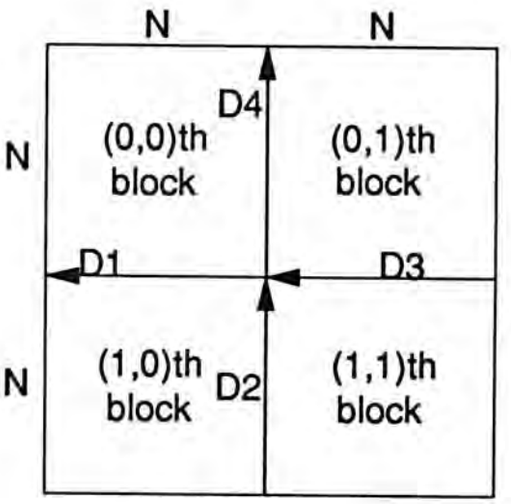

Fig.4.3 The four blocks and edge difference vectors considered in Edge Discriminator.

The DC coefficient which represents the mean of a block is first calculated and subtracted from the pixels within the block. As described in chapter 3, the four edge difference vectors D_1, D_2, D_3 and D_4 can be found and minimized by condition of minimum edge difference. With a_{00}, the mean of $(0,0)^{th}$ block, set equals to m_a, it has been shown [CHAMc84] that the estimated means are given by :

$$a_{10} = [s(4) + s(3) - s(2) + 3s(1)] / 4 + m_a \quad (4.1a)$$

$$a_{11} = [s(4) + s(3) + s(2) + s(1)] / 2 + m_a \quad (4.1b)$$

$$a_{01} = [3s(4) - s(3) + s(2) + s(1)] / 4 + m_a \quad (4.1c)$$

where

$$m_a = [(b_{00}+b_{01}+b_{10}+b_{11}) - (a_{01}+a_{10}+a_{11})] / 4$$

s(p) is the average of elements in D_p, $p \in [1,4]$.

The value of m_a is chosen such that the average value of the 2Nx2N blocks remains unchanged. From the derivation of estimated means, a_{kl}, it can be seen the edge differences, after adding a_{kl} to corresponding blocks, will be minimum. When the original block has only uniform change, the original edge differences should be small and hence the estimation means are close to original. If the original block has large activity or high contrast edge, the original edge difference should be large and the estimation by minimizing edge difference would give large error. Hence, the accuracy of estimation depends on whether the four adjacent blocks contain high activities or not. This phenomenon can be used to discriminate whether a block contain high contrast edge or not. Therefore, an Edge Discriminator (ED) criterion is formed as follow :

If $|a_{k,l} - b_{k,l}| < t$ for all (k,l), then merge

else do not merge.

It can be seen that the ED criterion takes the same form as Chen's MDD criterion and requires only addition/subtraction and arithmetic shift to complete the estimation.

4.4 Simulation Results

Computer simulation is carried out to compare the two variable block size coding systems. The test images have resolution of 8 bits per pixel and size 256x256. The parameters are chosen to be the same as that in [CHEN89]. The largest and smallest block sizes allowed are 16x16 and 4x4 respectively. The decision threshold t is 10 and the quantization values are 1,3 and 6 for block sizes of 16x16, 8x8, 4x4 respectively. The quantized coefficients are then Huffman coded in a similar way as in [CHENp84]. Comparison is made with Chen's system by using MSE, eq.(3.20), as criterion.

Fig.4.4 shows the simulation results using four test images : LENNA, PEPPERS, SAILBOAT and BABOON. It can be seen that VBS DCT transform coding system using the ED criterion produces lesser MSE with average bit rates tested in the range of 1.0 bpp to 1.5 bpp.

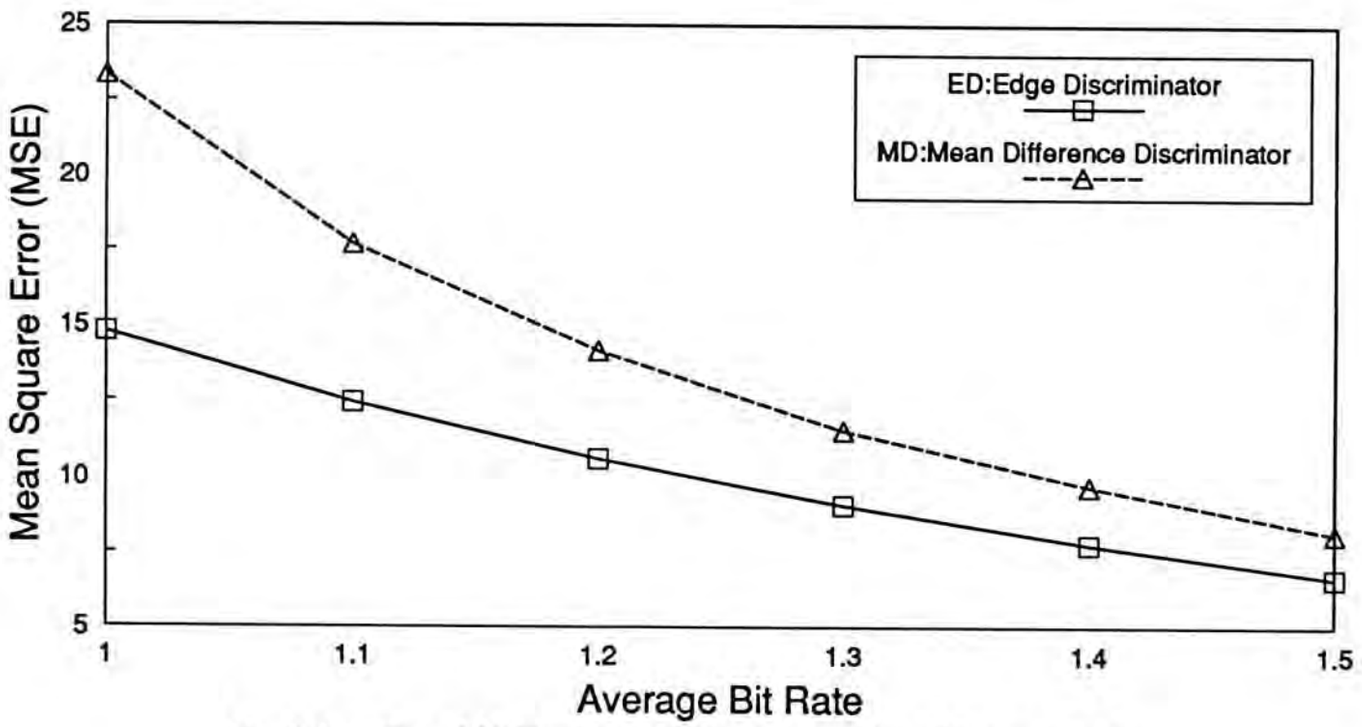

Fig.4.4a. The MSEs due to the use of the ED and MD in a Variable Block Size DCT Transform System for image LENNA

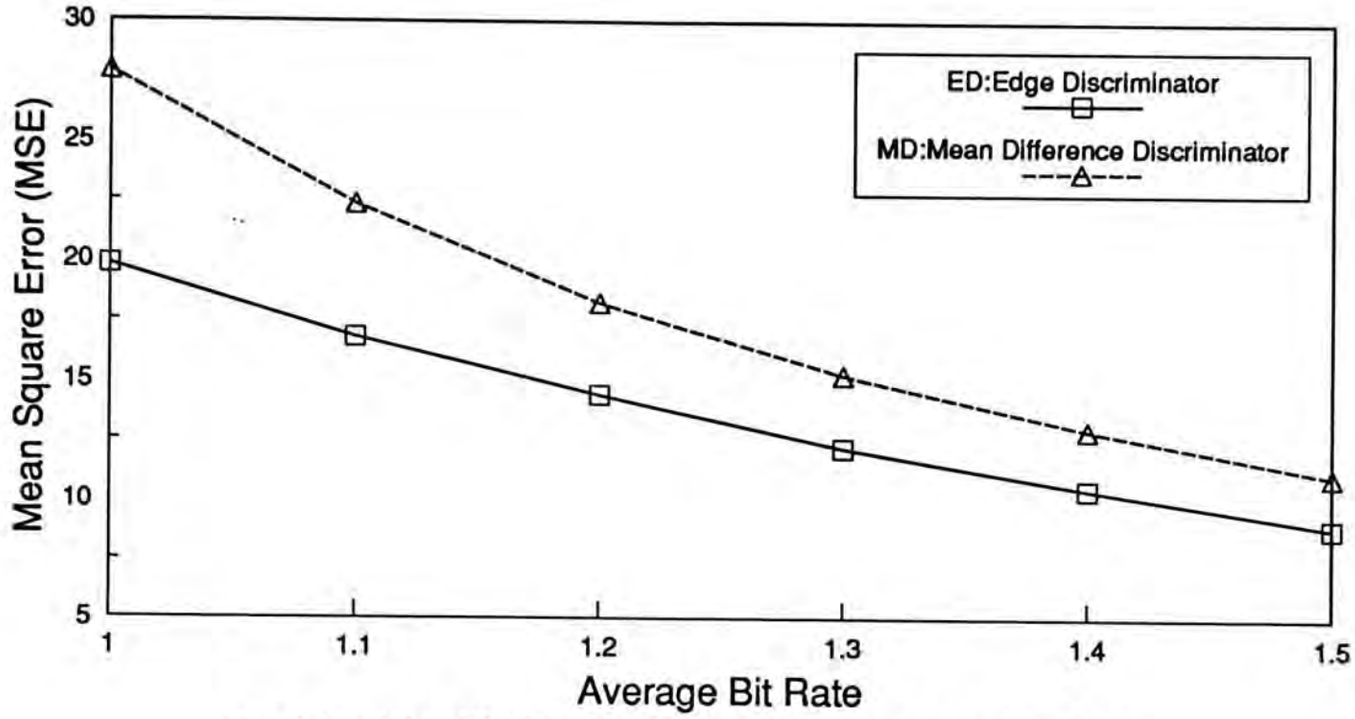

Fig.4.4b. The MSEs due to the use of the ED and MD
in a Variable Block Size DCT Transform System
for image PEPPERS

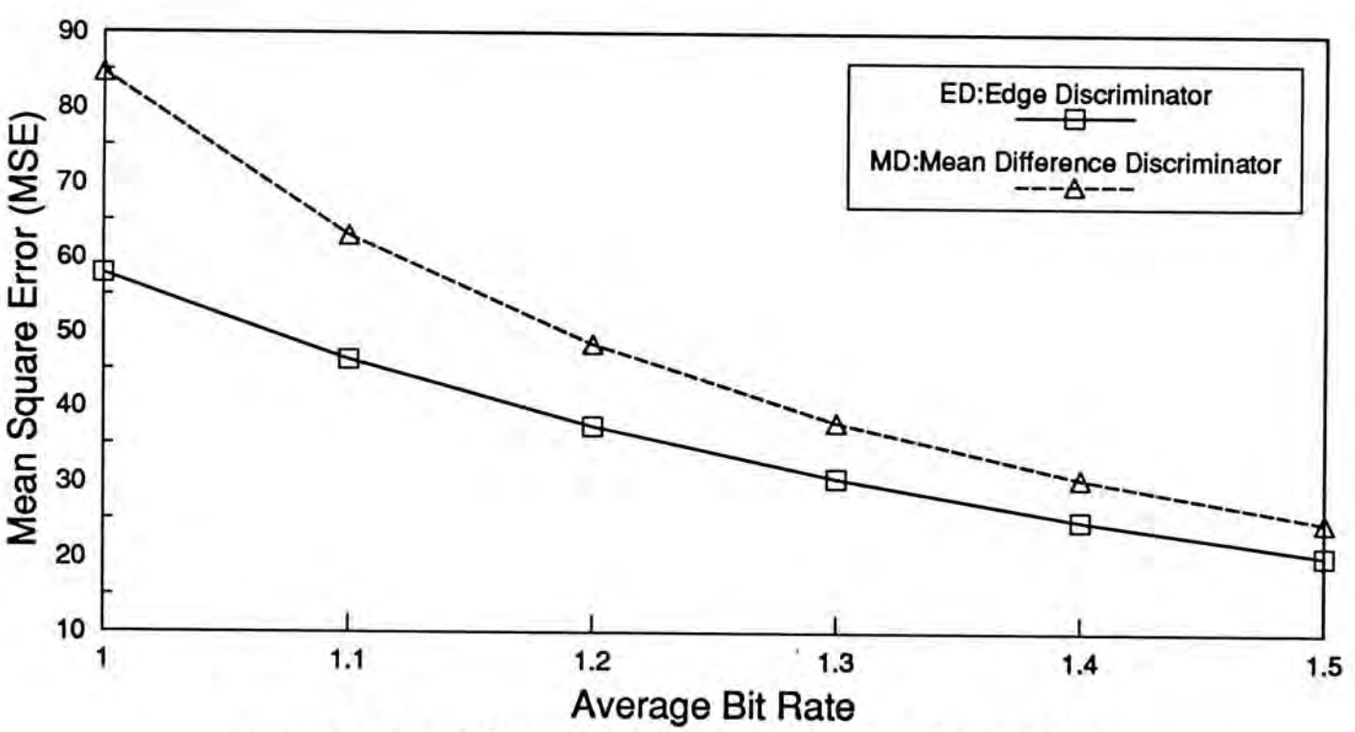

Fig.4.4c. The MSEs due to the use of the ED and MD
in a Variable Block Size DCT Transform System
for image SAILBOAT

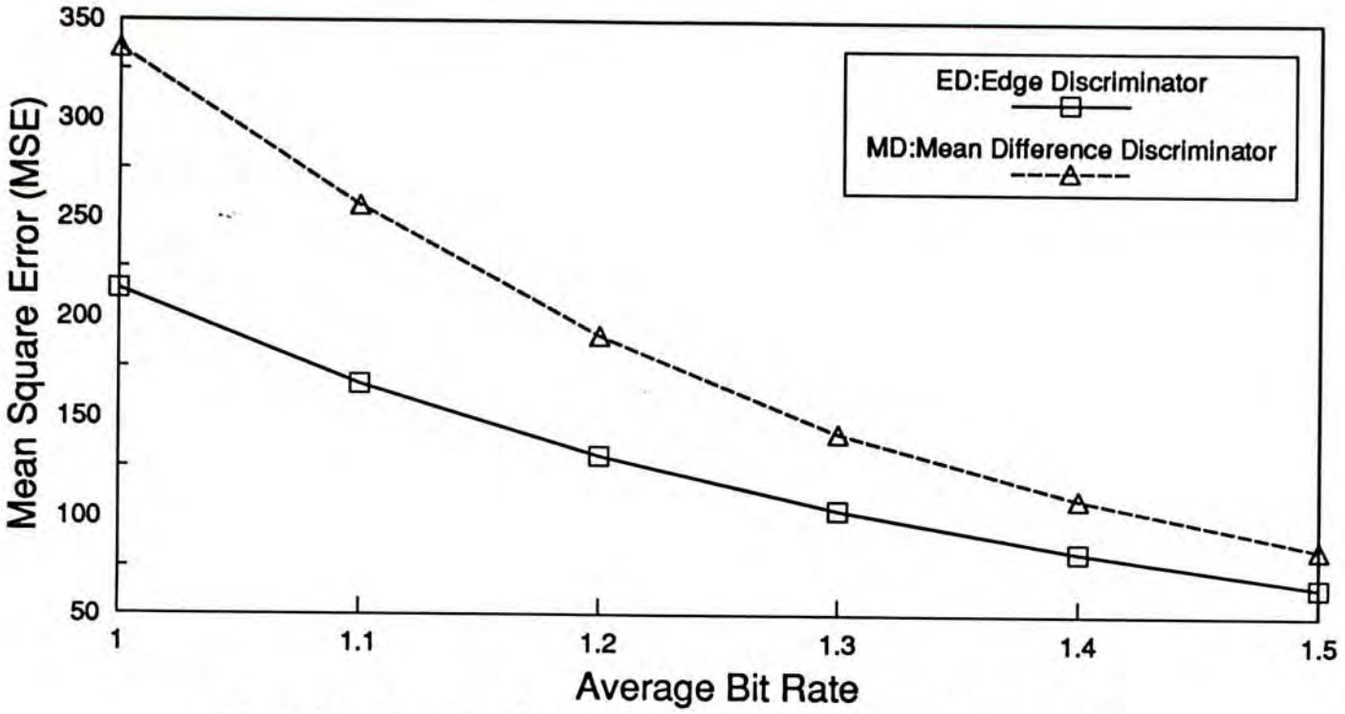

Fig.4.4d. The MSEs due to the use of the ED and MD in a Variable Block Size DCT Transform System for image BABOON

Fig.4.5 illustrates the resulting images of LENNA and BABOON after being processed by a variable block size coding scheme using the two decision criteria for bit rate 1.0 bpp and 1.5 bpp. It can also be seen that variable block size technique using the ED criterion produces better visual quality than that using the MDD criterion.

(a) LENNA, ED, 1.0 bpp (b) LENNA, MDD, 1.0 bpp

Fig.4.5 Images after processed by the VBS scheme, using ED and MDD as criteria.

(c) LENNA, ED, 1.5 bpp

(d) LENNA, MDD, 1.5 bpp

(e) BABOON, ED, 1.0 bpp

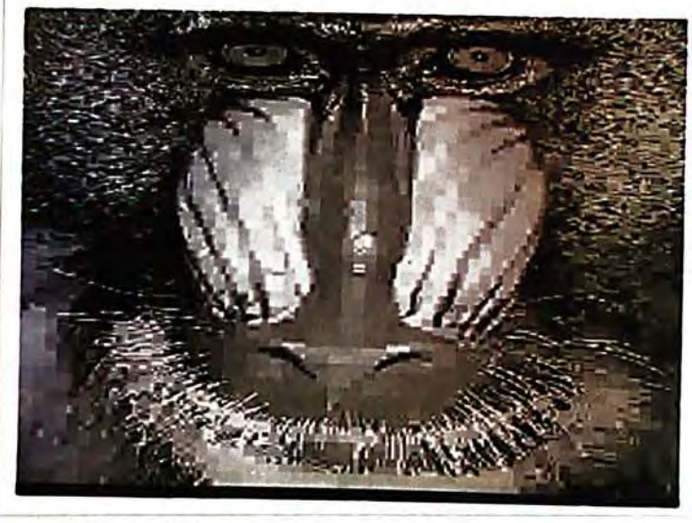

(f) BABOON, MDD, 1.0 bpp

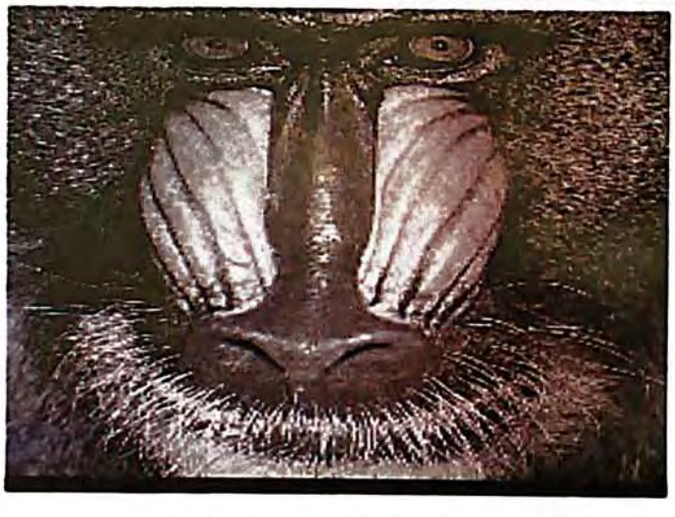

(g) BABOON, ED, 1.5 bpp

(h) BABOON, MDD, 1.5 bpp

Fig.4.5 Images after processed by the VBS scheme, using ED and MDD as criteria.

4.5 Discussion and Conclusion

The limitation of conventional fixed block size transform coding system has been discussed. Variable block size transform coding technique has been proven [CHEN89] to be capable of enhancing performance of a fixed block size transform coding system. In a VBS coding system, a criterion has to be used for determining the block size. Ideally, the criterion should be able to discriminate those blocks with uniform changes from those blocks with high activities. If the decision criterion can predict precisely whether the blocks contain high activities, the performance of coding system can be greatly improved. In [CHEN89], a variable block size transform coding system using mean difference discriminator as a decision criterion has been proposed. This criterion, however, cannot precisely estimate whether a block contain high contrast edge or not. Hence we propose a new decision criterion, the Edge Discriminator (ED) criterion, which involves estimation of means of local subblocks and maintains the same form of criterion as Mean Difference Discriminator (MDD) criterion. By eq.(3.17) - (3.19), it can be seen that the ED criterion requires only addition/subtraction and arithmetic shift and 8N+5 extra addition/subtractions are needed for block size N. Simulation results have been obtained for images with average bit rate ranging from 1.0 bpp to 1.5 bpp. For all these bit rates tested, the results show that an adaptive variable block size coding scheme employing the Edge Discriminator have better performance, both in MSE and visual quality.

Thus it can be concluded that the decision criterion in determining the block size is vital to the success of a VBS coding system. From simulation results given, we can say that the ED criterion is an more effective criterion than MDD criterion in determining the block size and hence is a better decision criterion for a VBS coding system.

Part of the results in this chapter have been published in [SEEc91].

5. ENHANCEMENT OF JPEG INTERNATIONAL STANDARD

5.1 Introduction

Recently, the Joint Photographic Experts Group (JPEG), which is a sub-working group of both the CCITT and ISO, is drafting an international standard for compression of still images [JPEG90]. The JPEG scheme is basically a transform coding system which divides an input image into 8x8 blocks. At the encoder, each input block of data first undergoes a 2-D Discrete Cosine Transform (DCT) and the transform coefficients are uniformly quantized. The quantized AC coefficients are coded using run-length and Huffman coding. The DC coefficients are coded using DPCM with the prediction error coded using Huffman coding.

As the JPEG scheme will become an international standard for still image coding, further enhancement of coding performance should be based on the JPEG scheme. In this chapter, we will study the basic JPEG scheme, which will be described in section 5.2. By using some of the techniques in previous chapters, we try to enhance the performance of the basic JPEG scheme. The following objectives are to be achieved in enhancing the JPEG scheme.

1. The enhanced JPEG scheme should have better performance under the criteria of both less MSE and better visual quality.

2. The enhanced JPEG scheme should be very similar to the basic JPEG scheme such that it can be easily incorporated as enhanced feature in existing product.

3. The basic JPEG scheme uses a rather simple algorithm that it can be easily implemented in hardware. The enhanced JPEG scheme should retain the simplicity of the basic JPEG scheme. In particular, memory is the other concern and the enhanced JPEG scheme should remain a one-pass process. In other words, there is no need for extra memory to store the images for a second pass in processing the images before they can be sent.

4. An image coded using the enhanced JPEG scheme is the same as the basic JPEG scheme but requires less bits for representation.

Two aspects in the basic JPEG scheme will be modified for performance enhancement. Firstly, the encoding of DC coefficients in basic JPEG scheme is examined and it is found that by employing the Element Estimation described in chapter 3, the performance of the coding scheme can be enhanced. Secondly, we have seen in chapter 4 that the VBS technique can be used to enhance the performance of a coding system. This VBS technique will again be used in enhancing the basic JPEG scheme.

In the basic JPEG scheme, the technique of DPCM is used to encode the DC coefficients of each block. The predictor used is a previous element predictor. The advantage of this predictor is that its operation is simple and only one addition/subtraction is required. However, it does not fully exploit the redundancy between DC coefficients of adjacent blocks. Hence we will propose a Minimum Edge Difference (MED) predictor to enhance the encoding performance.

In the JPEG scheme, the block size used to partition an image is fixed. By taking into account that images have different statistics over different areas, the VBS technique should be used for adapting the block size according to local activities. The VBS technique using Edge Discriminator as described in chapter 4 will be employed to enhance the performance of the basic JPEG scheme. Several schemes will be examined to see the effect of applying VBS technique to the basic JPEG scheme. Finally, a scheme with promising improvement will then be combined with the use of MED predictor for further enhancement.

In the following section, the basic JPEG scheme will be briefly described. The use of a more efficient predictor for the DC coefficients will be described in section 5.3 and the use of the variable block size technique will be described in section 5.4. Finally, conclusion will be drawn in section 5.5.

5.2 The basic JPEG international standard

The JPEG international standard is a proposed scheme for achieving image compression and decompression. The proposed JPEG standard offers a continuous range of compression to reduce the transmission and storage requirements of large images. The broad

scope and the variety of targets to be achieved result in a three-part JPEG algorithm definition : the basic system, the extended system, and the special function for lossless encoding. The basic system is mandatory, while the extended system adds features such as sophisticated coding, lossless transmission, and progressive transmission. Here we will only concern with the basic system of JPEG scheme, which utilizes the techniques of transform coding and DPCM coding.

The JPEG scheme is intended to be used for monochrome or colour images. For colour image, each colour (R,G,B) can be handled as separate components. However, better compression result can be achieved if the colour components are independent, such as YUV, where most of the information is concentrated in the luminance component (Y) and less in the chrominance components (U,V). Therefore, for a colour image, the input R,G,B components are first converted into Y,U,V components by using a linear transformation as follow [CUBE90] :

$$\begin{bmatrix} Y \\ U \\ V \end{bmatrix} = \begin{bmatrix} 0.299 & 0.587 & 0.114 \\ -0.169 & -0.3316 & 0.5 \\ 0.5 & 0.4186 & -0.0813 \end{bmatrix} \cdot \begin{bmatrix} R \\ G \\ B \end{bmatrix} \tag{5.1}$$

Another advantage of using YUV colour space is that chrominance components (U and V) need not be specified as frequently as the luminance component (Y). In the JPEG scheme, the spatial resolution of the U and V components is reduced by discarding every other U and V elements. As a result, a further data reduction of 3 to 2 is obtained by transforming RGB into YUV.

After colour space conversion, each component can then be independently processed by the JPEG system. A block diagram of the basic JPEG system is shown in Fig.5.1.

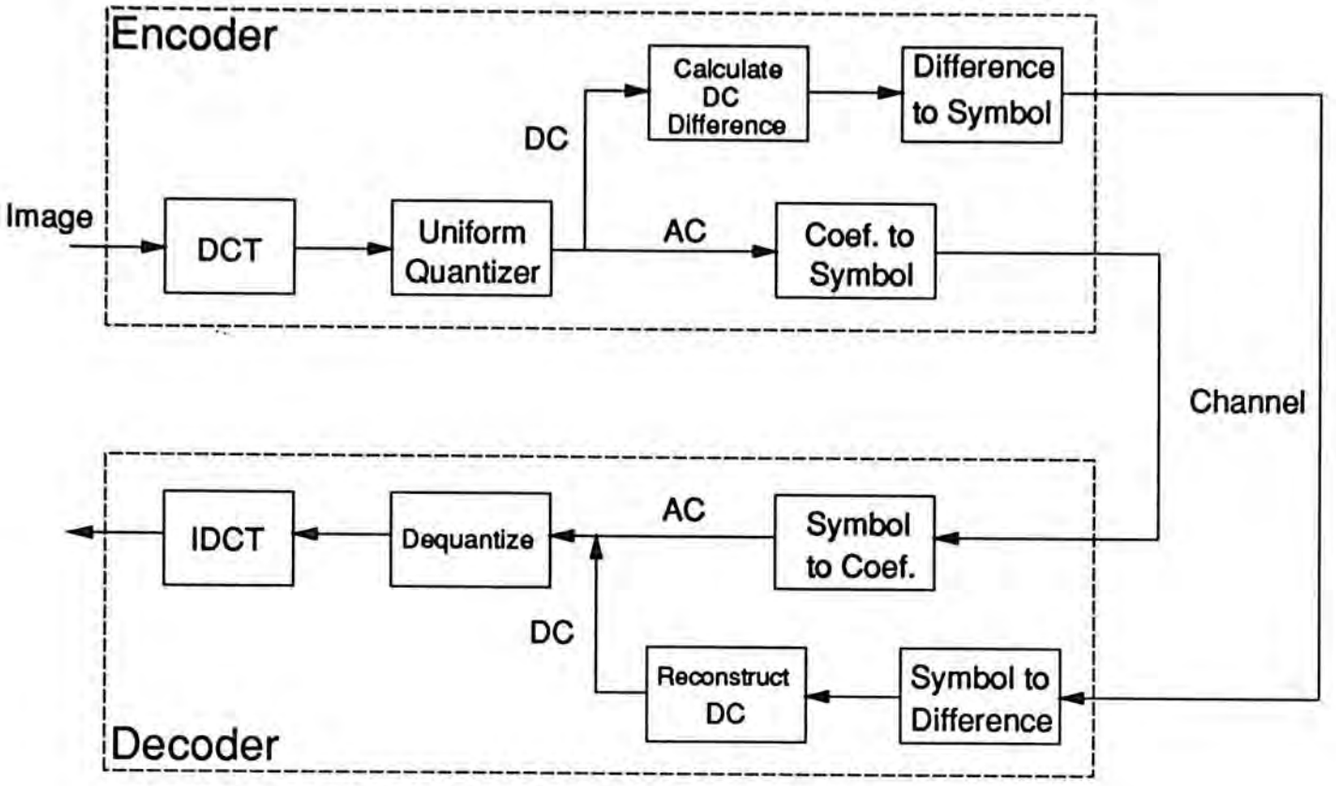

Fig.5.1 A Block Diagram of the Basic JPEG System

Both encoder and decoder in JPEG system consist of three parts which are the DCT, quantization and Huffman coding. They are briefly described as follow :

5.2.1. Level Shift and Discrete Cosine Transform

At the encoder, each component of an input image is first divided into non-overlapping 8x8 blocks. Before being processed by the forward DCT, all the input pixels are level shifted by subtracting 2^{p-1}, where p is the precision of image pixel and usually equals to 8. Then each block undergoes a 2-D DCT, converting pixel elements into transform coefficients as follow :

$$Y(u,v) = \frac{1}{4} K(u)K(v) \sum_{i=0}^{7} \sum_{j=0}^{7} x(i,j) \cos\frac{(2i+1)u\pi}{16} \cos\frac{(2j+1)v\pi}{16} \qquad (5.2)$$

where $i,j,u,v \in [0,7]$

$x(i,j)$ = $(i,j)^{th}$ element in a 8x8 image block

$Y(u,v)$ = $(u,v)^{th}$ element in a 8x8 DCT coefficient matrix

$$K(u) = \begin{cases} 1/\sqrt{2} & \text{for} \quad u = 0 \\ 1 & \text{for} \quad u \neq 0 \end{cases}$$

At the decoder, the dequantized coefficients will go through the inverse DCT as in eq.(5.3)

$$x(i,j) = \frac{1}{4} \sum_{u=0}^{7} \sum_{v=0}^{7} K(u)K(v)\, Y(u,v) \cos\frac{(2i+1)u\pi}{16} \cos\frac{(2j+1)v\pi}{16} \tag{5.3}$$

Finally, 128 are added to the pixels to obtain the reconstructed image.

5.2.2. Uniform Quantization

At the encoder, each DCT coefficient, Y(u,v), is uniformly quantized with a quantization value, Q(u,v), as shown in Fig.5.2.

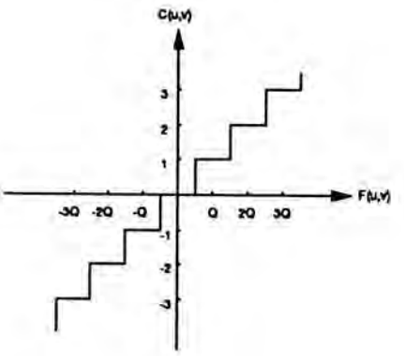

Fig 5.2 Uniform Quantization of Transform Coefficients.

In mathematical form,

$$C(u,v) = \left\lfloor \frac{Y(u,v)}{Q(u,v)} \right\rfloor \tag{5.4}$$

where C(u,v) = quantized DCT coefficients

Q(u,v) = quantization value for $(u,v)^{th}$ coefficient

$\lfloor . \rfloor$ is the rounding operator

At the decoder, dequantization[1] is similarly carried out to obtain the dequantized transform coefficients :

$$Y'(u,v) = C(u,v) \times Q(u,v) \tag{5.5}$$

where $Y'(u,v)$ is the dequantized DCT coefficient.

The quantization of each 64 coefficients are separately specified by a quantization matrix of 64 independent values and can be varied according to the statistics of image being quantized and the sensitivity of human eye for different coefficients. Two default quantization matrices, one for the luminance component and the other for the chrominance components, are specified and given in eq.(5.6).

Q_1 = quantization matrix for luminance component

$$= \begin{bmatrix} 16 & 11 & 10 & 16 & 24 & 40 & 51 & 61 \\ 12 & 12 & 14 & 19 & 26 & 58 & 60 & 55 \\ 14 & 13 & 16 & 24 & 40 & 57 & 69 & 56 \\ 14 & 17 & 22 & 29 & 51 & 87 & 80 & 62 \\ 18 & 22 & 37 & 56 & 68 & 109 & 103 & 77 \\ 24 & 35 & 55 & 64 & 81 & 104 & 113 & 92 \\ 49 & 64 & 78 & 87 & 103 & 121 & 120 & 101 \\ 72 & 92 & 95 & 98 & 112 & 100 & 103 & 99 \end{bmatrix} \tag{5.6a}$$

Q_2 = quantization matrix for chrominance component

$$= \begin{bmatrix} 17 & 18 & 24 & 47 & 66 & 99 & 99 & 99 \\ 18 & 21 & 26 & 66 & 99 & 99 & 99 & 99 \\ 24 & 26 & 56 & 99 & 99 & 99 & 99 & 99 \\ 47 & 66 & 99 & 99 & 99 & 99 & 99 & 99 \\ 99 & 99 & 99 & 99 & 99 & 99 & 99 & 99 \\ 99 & 99 & 99 & 99 & 99 & 99 & 99 & 99 \\ 99 & 99 & 99 & 99 & 99 & 99 & 99 & 99 \\ 99 & 99 & 99 & 99 & 99 & 99 & 99 & 99 \end{bmatrix} \tag{5.6b}$$

---

1 The term dequantization is used in the JPEG proposal.

The $(u,v)^{th}$ element in Q_1 and Q_2 is thus the quantization value for $(u,v)^{th}$ luminance and chrominance transform coefficients respectively.

5.2.3. Coefficient Coding

At the encoder, after coefficient quantization, the 2-D array of quantized AC coefficients is first rearranged into a 1-D array, using a zigzag scan ordering, as shown in Fig.5.3.

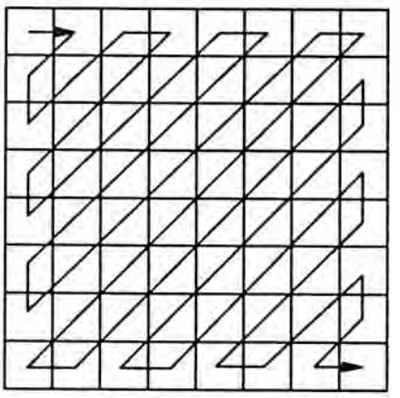

Fig.5.3 Zigzag scan path

Each nonzero quantized AC coefficient in the vector of zigzag ordered coefficients is then encoded in combination with the length, or so-called run-length, of preceding zero valued AC coefficients. The composite value of run-length and amplitude of the quantized AC coefficient are then Huffman coded. For the DC coefficients, a 1-D 'previous element predictor' is used in which the predicted value of the DC coefficient of current block is simply the DC coefficient of previous block.

$$\hat{DC}_{k,l} = DC_{k,l-1} \tag{5.7}$$

The difference $d_{k,l}$ between predicted DC coefficient and quantized DC coefficient is then Huffman coded using a default Huffman table in [JPEG90].

5.3 Efficient DC Coefficients Encoding

In the basic JPEG system, the predictor used is a simple 'previous element predictor' which uses the DC coefficient of previous block as the predicted DC coefficient of the current block. This simple DPCM predictor is very effective for prediction of adjacent pixel element as the adjacent element correlation coefficient between pixel elements is close to unity. However, the correlation coefficient of DC coefficients between adjacent blocks is not as high as that between spatial pixel elements, so the simple DPCM predictor is not very effective in predicting the DC coefficients. In this section, a Minimum Edge Difference (MED) predictor is proposed for more efficient encoding of the DC coefficients. It requires only low extra computation and can be easily incorporated into the basic JPEG scheme. The prediction is done by minimizing the edge difference between the current block and the adjacent blocks, as shown in Fig.5.4. By the use of the MED predictor, we can obtain images with same quality as the basic JPEG scheme but requiring less bit for representation. Some other common predictors are also compared with the MED predictor. From the simulation result, it can be shown that the MED predictor requires minimum number of bits for representing the difference between predicted and original DC coefficients and hence it is the most effective predictor among those tested. The details are described as follow.

5.3.1 The Minimum Edge Difference (MED) Predictor

The Minimum Edge Difference predictor is basically the same as the element estimator in Cham's DC coefficient restoration scheme [CHAMc84] and has been described in chapter 3.

In the MED predictor, the vertical and horizontal edge difference vectors, as shown in Fig.5.4, are used.

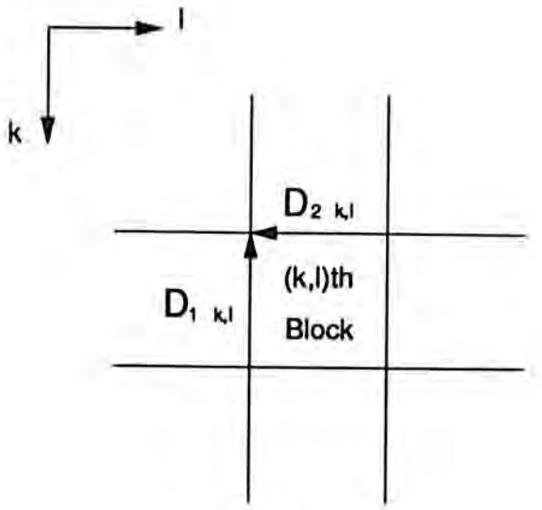

Fig.5.4 The two edge difference vectors considered in the MED predictor

The edge difference vectors indicate the change between pixels along the edge of adjacent blocks. Since the correlation between adjacent pixels is usually large, the DC coefficients can be predicted by minimizing these edge difference vectors between the current and adjacent blocks. Hence, as described in chapter 3, the predicted value of the DC coefficient is :

$$\hat{DC}_{k,l} = \frac{1}{2} \times \sum_{p=1}^{2} \sum_{m=0}^{N-1} d(p,m)_{k,l} \tag{5.8}$$

where $d(p,m)_{k,l}$ is the m^{th} element of the vector $D_{p\ k,l}$.

The DC difference signal $d_{k,l}$ is then Huffman coded in the same way as the basic JPEG scheme, where

$$d_{kl} = DC_{kl} - \hat{DC}_{kl} \tag{5.9}$$

5.3.2 Simulation Results

To demonstrate the bit rate reduction of the modified JPEG scheme using the MED predictor, computer simulations have been carried out to evaluate the performance of the

predictor on several colour images which are of size 256x256 pixels and 8-bits resolution for each of the red (R), green (G) and blue (B) components. In the evaluation of the system performance, the MSE defined in eq.(3.20) is used.

Table 5.1 and 5.2 show the simulation results for colour images by using the original JPEG's predictor and the MED predictor.

Picture	LENNA			PEPPERS			SAILBOAT			BABOON		
Bit Rate	1.00	0.75	0.50	1.00	0.75	0.50	1.00	0.75	0.50	1.00	0.75	0.50
MSE	80.7	101.8	147.1	132.9	165.0	238.3	259.6	310.1	425.2	520.4	590.1	704.1

Table 5.1 Simulation Results for basic JPEG Scheme

Picture	LENNA			PEPPERS			SAILBOAT			BABOON		
Bit Rate	0.949	0.711	0.473	0.951	0.712	0.474	0.972	0.728	0.486	0.974	0.732	0.487
MSE	80.7	101.8	147.1	132.9	165.0	238.3	259.6	310.1	425.2	520.4	590.1	704.1

Table 5.2 Simulation Results for JPEG Scheme with MED Predictor

For the basic JPEG system, the images tested are coded at 0.5, 0.75 and 1.00 bpp. By using the MED predictor, the same coded images of LENNA and PEPPERS can be represented using only about 0.47, 0.71 and 0.95 bpp respectively. That is equivalent to about 5% bit rate reduction over the basic JPEG scheme. For the image SAILBOAT and BABOON, the same coded images can be represented using about 0.487, 0.73 and 0.97 bpp, equivalent to about 3% bit rate reduction over the basic JPEG scheme. Thus, by incorporating a MED predictor into the basic JPEG scheme, we can obtain 3% to 5% bit rate reduction without affecting the image quality and extra computation required is small.

For subjective quality comparison, the original colour images of LENNA and BABOON are shown in Fig.5.5 and the images LENNA and BABOON after being processed by the basic JPEG scheme, are shown in Fig.5.6. The images obtained by using the MED predictor have the same quality as those by using the basic JPEG scheme.

(a) LENNA

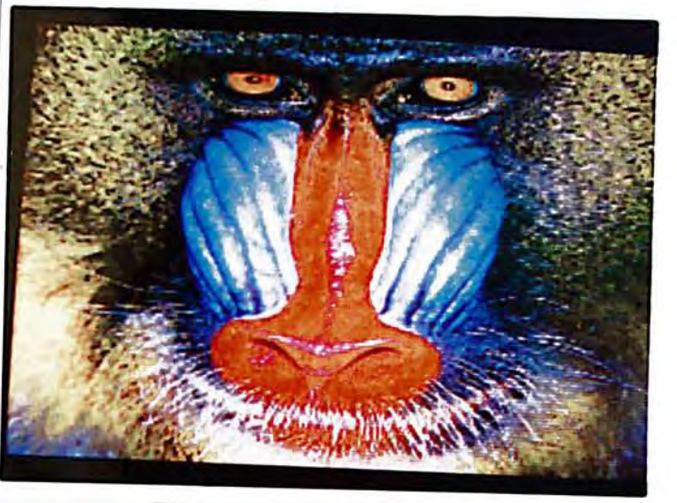

(b) BABOON

Fig.5.5 Original images

(a) LENNA, 0.5 bpp

(d) BABOON, 0.5 bpp

(b) LENNA, 0.75 bpp

(e) BABOON, 0.75 bpp

(c) LENNA, 1.0 bpp

(f) BABOON, 1.0 bpp

Fig.5.6 Images after processed by the basic JPEG scheme

5.3.3 Pixel Domain Predictors

To further demonstrate the suitability and effectiveness of the proposed MED predictor for encoding the DC coefficients, we compare it with several predictors designed based on the criterion of minimizing the mean square prediction error [BRAINp90]. To predict the DC coefficient X of a current block, we can use the DC coefficient of previous blocks, as shown in Fig 5.7. The predicted DC coefficient $\hat{X}$ is

$$\hat{X} = a \cdot A + b \cdot B + c \cdot C + d \cdot D \tag{5.10}$$

where A,B,C,D are DC coefficients of previous blocks and a,b,c,d are the corresponding prediction coefficients.

In [BRAINp90], tests have been carried out to find the optimum prediction coefficients a,b,c,d. Several predictors have been obtained by making use some of the DC coefficients A,B,C,D, based on the criterion of minimizing the mean square prediction error. These predictors are characterized by their prediction coefficients and are listed in Table 5.3. To compare the effectiveness of these predictors and the MED predictor, DC coefficients of test images are predicted using all these predictors and the differences are Huffman coded using the default table given in the basic JPEG scheme. Predictor P0 is the simple previous element horizontal predictor used in the basic JPEG scheme. The quantized AC coefficients are coded with the same number of bits and the number of bits required to code the quantized DC coefficients for different predictors are shown in Table 5.4.

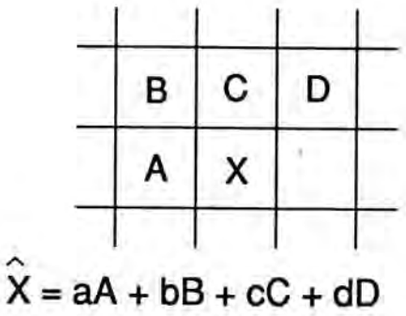

Fig.5.7 Tap Nomenclature for predicting sample block X (A,B,C and D are the DC coefficients of blocks and a,b,c and d are the corresponding prediction coefficients)

Predictor	Predictor Coefficients			
	a	b	c	d
P0	1	0	0	0
P1	1/2	0	1/2	0
P2	1	-1/2	1/2	0
P3	3/4	-3/8	5/8	0
P4	13/16	-5/16	1/2	0
P5	7/8	-1/2	1/2	1/8
P6	1/2	1/8	1/4	1/8
P7	3/4	-1/4	3/8	1/8

Table 5.3 Prediction coefficients of the eight predictors

	LENNA			PEPPERS			SAILBOAT			BABOON		
Predictor	MSE =80.7	MSE =101.8	MSE =147.1	MSE =132.9	MSE =165.0	MSE =238.3	MSE =259.6	MSE =310.1	MSE =425.2	MSE =520.4	MSE =590.1	MSE =704.1
P0	10868	9654	8224	10796	9557	8162	9223	8272	7202	8971	8228	7352
P1	9159	8165	7135	9578	8550	7440	8403	7596	6750	7940	7431	6764
P2	9228	8240	7201	9721	8686	7537	8406	7620	6788	8045	7493	6828
P3	8886	7967	6935	9497	8457	7343	8329	7554	6739	7835	7232	6636
P4	9335	8250	7239	9833	8790	7656	8778	7990	7148	8035	7495	6818
P5	8945	7990	6995	9538	8516	7410	8419	7595	6779	7891	7301	6683
P6	9413	8434	7258	9743	8666	7543	8495	7661	6760	8035	7519	6841
P7	9108	8175	7106	9606	8274	7446	8413	7580	6768	7936	7382	6737
MED	7515	7092	6480	7594	7089	6483	7392	6827	6308	7282	7015	6503

Table 5.4 Number of bits required to code the DC coefficients for different predictors when the MSE is fixed

The results show that for the same MSE, employing the MED predictor requires the minimum number of bits to represent all four images.

5.3.4 Discussion and Conclusion

The basic JPEG scheme is basically a transform coding system that at the transmitter, an input image is transformed by the DCT and the transform coefficients are uniformly quantized. The AC coefficients are run-length and Huffman coded. The DC coefficients are encoded using a simple 'previous element predictor'. This predictor is not quite effective due to the not-high enough correlation between DC coefficients of adjacent blocks. Therefore, a Minimum Edge Difference Predictor is proposed to enhance the performance of the basic JPEG system. It has the advantages that the MED predictors requires only low additional computation requirement. 16 additions are required in predicting the DC coefficient of each block. Thereafter, the prediction error is Huffman coded using the same table given in [JPEG90]. Thus it can maintain the simplicity of the JPEG scheme and can be easily incorporated in existing products as enhanced feature. Moreover, the MED predictor only require information from previous blocks and can still be implemented in one-pass. Simulation results show that the coded images maintain the same quality as the basic JPEG scheme and there is about 3 to 5% bit rate reduction when using the MED predictor. By comparing to other predictors listed in Table 5.4, the superiority of MED predictor is also demonstrated.

Part of the results in this section have been published in [SEElc91].

5.4 JPEG Scheme Using Variable Block Size Technique

Variable block size technique has been used in chapter 4 to improve performance of a coding system over that of a fixed block size system. This technique will now again be used to enhance the performance of the basic JPEG system. Edge Discriminator described in chapter 4 will be used to determine suitable block size for different area of an image. Five schemes using the VBS technique have been examined and the results of their performance are obtained. They are described in following section.

5.4.1 Scheme 1

In this scheme, the technique of variable block size is used instead of fixed block size in original JPEG scheme. The Edge Discriminator is used to determine whether a block should be encoded as a single 16x16 block, four 8x8 blocks, sixteen 4x4 blocks or other combination. After block size determination, the block will undergo the basic JPEG scheme similarly. The quantized DC and AC coefficients are then similarly Huffman coded using the same default table in [JPEG90].

In the basic JPEG scheme, only order-8 quantization matrices are given. To incorporate the VBS technique into the JPEG scheme, order-4 and order-16 quantization matrices have to be determined. Extensive search may be needed to find the optimum quantization matrices. However, it takes a long time for searching. So we try to obtain the order-4 and order-16 quantization matrices from the given order-8 quantization matrix. This can be done by finding the relationship between order-N and order-2N quantization matrices. As one of the factors in determining quantization values is the variance of the transform coefficients, we first investigate the relationship between variance of NxN and 2Nx2N transform coefficients.

In JPEG scheme, the forward DCT is defined as

$$T(N,p,q) = \frac{4 \cdot K(p)}{N} \cdot \cos\frac{(2q+1)p\pi}{2N} \tag{5.11a}$$

$$T(2N,r,s) = \frac{4 \cdot K(r)}{2N} \cdot \cos\frac{(2s+1)r\pi}{4N} \tag{5.11b}$$

where $T(N,p,q)$ is the $(p,q)^{th}$ element of NxN DCT transform matrix, $p,q \in [0,N-1]$, $r,s \in [0,2N-1]$.

When $r = 2p$ and $p \in [0,N-1]$,

$$T(2N,2p,s)=\frac{4\cdot K(2p)}{2N}\cdot\cos\frac{(2s+1)2p\pi}{4N}$$

$$=\frac{4\cdot K(p)}{2N}\cdot\cos\frac{(2s+1)p\pi}{2N}$$

If $s \in [0,N-1]$,

$$T(2N,2p,s)=\frac{1}{2}T(N,p,s) \tag{5.12}$$

If $s \in [N,2N-1]$, let $s' = 2N-s-1$,

$$T(2N,2p,s)=\frac{4\cdot K(p)}{2N}\cdot\cos\frac{[2(2N-s'-1)+1]\,p\pi}{2N}$$

$$=\frac{4\cdot K(p)}{2N}\cdot\cos\frac{(2s'+1)p\pi}{2N}$$

So,

$$T(2N,2p,s)=\frac{1}{2}T(N,p,2N-s-1) \tag{5.13}$$

$$T(2N,2p,s)=T(2N,2p,2N-s-1) \tag{5.14}$$

When $r = 2p+1$, $p \in [0,N-1]$, and if $s \in [N,2N-1]$, let $s' = 2N-s-1$,

$$T(2N,2p+1,s)=\frac{4\cdot K(2p+1)}{2N}\cdot\cos\frac{[2(2N-s'-1)+1]\,(2p+1)\pi}{4N}$$

$$=-\frac{2}{N}\cdot\cos\frac{(2s'+1)(2p+1)\pi}{4N}$$

So,

$$T(2N,2p+1,s)=-T(2N,2p+1,2N-s-1) \tag{5.15}$$

Eq.(5.12) and (5.13) show the relationship between basis vectors of [T(N)] and even basis vectors of [T($2N$)]. Eq.(5.14) and (5.15) show that the (2N-1)th dyadic symmetry exists in the basis vectors. Assume that a 2Nx2N block with covariance matrix C_x is transformed by [T($2N$)]. The variance of transform coefficient, where u,v $\in$ [0,2N-1], is :

$$\sigma_c^2(2N,u,v) = \sum_{i,j,p,q=0}^{2N-1} C_x(i,j;p,q)\,T(2N,u,i)\,T(2N,v,j)\,T(2N,u,p)\,T(2N,v,q) \quad (5.16)$$

Let $C_{abcd}(i,j;p,q) = C_x(i+aN,j+bN;p+cN,q+dN)$, where (a,b,c,d) $\in$ [0,1] and (i,j,p,q) $\in$ [0,N-1]. For simplicity, we drop the index i,j,p,q in C_x. If u = 2u', v = 2v' and u',v' $\in$ [0,N-1], by using eq.(5.12) and (5.13), eq.(5.16) becomes :

$$\begin{aligned}
\sigma_c^2(2N,2u',2v') = \frac{1}{16} \sum_{i,j,p,q=0}^{N-1} \{ & C_{0000}\,T(N,u',i)\,T(N,v',j)\,T(N,u',p)\,T(N,v',q) \\
& + C_{0001}\,T(N,u',i)\,T(N,v',j)\,T(N,u',p)\,T(N,v',N-q-1) \\
& + C_{0010}\,T(N,u',i)\,T(N,v',j)\,T(N,u',N-p-1)\,T(N,v',q) \\
& + C_{0100}\,T(N,u',i)\,T(N,v',N-j-1)\,T(N,u',p)\,T(N,v',q) \\
& + C_{1000}\,T(N,u',N-i-1)\,T(N,v',j)\,T(N,u',p)\,T(N,v',q) \\
& + C_{0011}\,T(N,u',i)\,T(N,v',j)\,T(N,u',N-p-1)\,T(N,v',N-q-1) \\
& + C_{0110}\,T(N,u',i)\,T(N,v',N-j-1)\,T(N,u',N-p-1)\,T(N,v',q) \\
& + C_{1100}\,T(N,u',N-i-1)\,T(N,v',N-j-1)\,T(N,u',p)\,T(N,v',q) \\
& + C_{1010}\,T(N,u',N-i-1)\,T(N,v',j)\,T(N,u',N-p-1)\,T(N,v',q) \\
& + C_{1001}\,T(N,u',N-i-1)\,T(N,v',j)\,T(N,u',p)\,T(N,v',N-q-1) \\
& + C_{0101}\,T(N,u',i)\,T(N,v',N-j-1)\,T(N,u',p)\,T(N,v',N-q-1) \\
& + C_{0111}\,T(N,u',i)\,T(N,v',N-j-1)\,T(N,u',N-p-1)\,T(N,v',N-q-1) \\
& + C_{1011}\,T(N,u',N-i-1)\,T(N,v',j)\,T(N,u',N-p-1)\,T(N,v',N-q-1) \\
& + C_{1101}\,T(N,u',N-i-1)\,T(N,v',N-j-1)\,T(N,u',p)\,T(N,v',N-q-1) \\
& + C_{1110}\,T(N,u',N-i-1)\,T(N,v',N-j-1)\,T(N,u',N-p-1)\,T(N,v',q) \\
& + C_{1111}\,T(N,u',N-i-1)\,T(N,v',N-j-1)\,T(N,u',N-p-1)\,T(N,v',N-q-1) \}
\end{aligned} \quad (5.17)$$

Eq.(5.17) can be simplified using eq.(5.14) and (5.15). Consider the following four cases :

(1) If u = 2u', u' = 2u"; v = 2v', v' = 2v"; u",v" ∈ [0,N/2-1],

$$\sigma_c^2(2N,4u",4v") = \frac{1}{16}\sum_{i,j,p,q=0}^{N-1}\sum\{C_{0000}+C_{0001}+C_{0010}+C_{0100}+C_{1000}+C_{0011}+C_{0110}+C_{1100} + C_{1010}+C_{1001}+C_{0101}+C_{0111}+C_{1011}+C_{1101}+C_{1110}+C_{1111}\} T(N,2u",i)\,T(N,2v",j)\,T(N,2u",p)\,T(N,2v",q)$$

(5.18a)

(2) If u = 2u', u' = 2u"; v = 2v', v' = 2v"+1; u",v" ∈ [0,N/2-1],

$$\sigma_c^2(2N,4u",4v"+2) = \frac{1}{16}\sum_{i,j,p,q=0}^{N-1}\sum\{C_{0000}-C_{0001}+C_{0010}-C_{0100}+C_{1000}-C_{0011}-C_{0110}\,C_{1100} + C_{1010}-C_{1001}+C_{0101}+C_{0111}-C_{1011}+C_{1101}-C_{1110}+C_{1111}\} T(N,2u",i)\,T(N,2v"+1,j)\,T(N,2u",p)\,T(N,2v"+1,q)$$

(5.18b)

(3) If u = 2u', u' = 2u"+1; v = 2v', v' = 2v"; u",v" ∈ [0,N/2-1],

$$\sigma_c^2(2N,4u"+2,4v") = \frac{1}{16}\sum_{i,j,p,q=0}^{N-1}\sum\{C_{0000}+C_{0001}-C_{0010}+C_{0100}-C_{1000}-C_{0011}-C_{0110}-C_{1100} + C_{1010}-C_{1001}+C_{0101}-C_{0111}+C_{1011}-C_{1101}+C_{1110}+C_{1111}\} T(N,2u"+1,i)\,T(N,2v",j)\,T(N,2u"+1,p)\,T(N,2v",q)$$

(5.18c)

(4) If u = 2u', u' = 2u"+1; v = 2v', v' = 2v"+1; u",v" $\in$ [0,N/2-1],

$$\sigma_c^2(2N,4u"+2,4v"+2)=\frac{1}{16}\sum_{i,j,p,q=0}^{N-1}\sum\sum\sum\{C_{0000}-C_{0001}-C_{0010}-C_{0100}-C_{1000}+C_{0011}+C_{0110}+C_{1100}$$
$$+C_{1010}+C_{1001}+C_{0101}-C_{0111}-C_{1011}-C_{1101}-C_{1110}+C_{1111}\}$$
$$T(N,2u"+1,i)\,T(N,2v"+1,j)\,T(N,2u"+1,p)\,T(N,2v"+1,q)$$

(5.18d)

Therefore, when u and v are even values, the variance $\sigma_c^2(2N,u,v)$ can be related with respect to the NxN basis pictures of DCT. The corresponding basis pictures are listed in the following table :

Variance	Basis Picture
$\sigma_c^2(2N,4u",4v")$	$\vec{T}(N,2u")\cdot\vec{T}(N,2v")$
$\sigma_c^2(2N,4u",4v"+2)$	$\vec{T}(N,2u")\cdot\vec{T}(N,2v"+1)$
$\sigma_c^2(2N,4u"+2,4v")$	$\vec{T}(N,2u"+1)\cdot\vec{T}(N,2v")$
$\sigma_c^2(2N,4u"+2,4v"+2)$	$\vec{T}(N,2u"+1)\cdot\vec{T}(N,2v"+1)$

Table 5.5 Variance $\sigma_c^2(2N)$ and their corresponding basis pictures

In summary, the variance of order-2N transform coefficients can be related to the basis pictures in order-N transform. We assume that the quantization values Q(*2N*,u,v) for order-2N transform coefficients are related to the quantization values Q(*N*,u,v) for order-N transform coefficients in a similar manner. To obtain the quantization matrix for order-2N transform coefficients, for even value of u and v, we set the ratio of quantization value Q(*2N*,2u',2v') and Q(*N*,u',v') equals to the ratio of $\sigma_c^2(2N,2u',2v')$ and $\sigma_c^2(N,u',v')$. For odd value of u or v, Q(*2N*,u,v) is linear interpolated between its adjacent quantization values.

Unfortunately, it is found that when all order-4 and order-16 quantization values are adjusted according to the ratio of variance, the simulation results are not satisfactory. Therefore, only some quantization values of low sequency coefficients are adjusted. After comparing the resulting coding performance of adjusting different number of quantization values, the following two quantization matrices for order-4 and order-16 are obtained which have on average the best performance :

$$Q(4) = \begin{bmatrix} 17 & 10 & 24 & 51 \\ 14 & 16 & 40 & 69 \\ 18 & 37 & 68 & 103 \\ 49 & 78 & 103 & 120 \end{bmatrix} \tag{5.19}$$

$$Q(16) = \begin{bmatrix} 15 & 7 & 7 & 8 & 10 & 13 & 16 & 20 & 24 & 32 & 40 & 46 & 51 & 56 & 61 & 66 \\ 8 & 8 & 12 & 10 & 12 & 15 & 18 & 21 & 25 & 37 & 49 & 52 & 56 & 57 & 58 & 58 \\ 7 & 12 & 8 & 11 & 14 & 17 & 19 & 23 & 26 & 42 & 58 & 59 & 60 & 58 & 55 & 53 \\ 11 & 11 & 10 & 13 & 15 & 18 & 22 & 27 & 33 & 45 & 58 & 61 & 65 & 60 & 56 & 56 \\ 14 & 14 & 13 & 15 & 16 & 20 & 24 & 32 & 40 & 49 & 57 & 63 & 69 & 63 & 56 & 50 \\ 14 & 15 & 15 & 17 & 19 & 23 & 27 & 36 & 46 & 59 & 72 & 73 & 75 & 67 & 59 & 59 \\ 14 & 16 & 17 & 20 & 22 & 26 & 29 & 40 & 51 & 69 & 87 & 84 & 80 & 71 & 62 & 53 \\ 16 & 18 & 20 & 25 & 30 & 36 & 43 & 51 & 60 & 79 & 98 & 95 & 92 & 81 & 70 & 70 \\ 18 & 20 & 22 & 30 & 37 & 47 & 56 & 62 & 68 & 89 & 109 & 106 & 103 & 90 & 77 & 64 \\ 21 & 25 & 29 & 37 & 46 & 53 & 60 & 67 & 75 & 91 & 107 & 107 & 108 & 96 & 85 & 85 \\ 24 & 30 & 35 & 45 & 55 & 60 & 64 & 73 & 81 & 93 & 104 & 109 & 113 & 103 & 92 & 82 \\ 37 & 43 & 50 & 58 & 67 & 71 & 76 & 84 & 92 & 102 & 113 & 115 & 117 & 107 & 97 & 97 \\ 49 & 57 & 64 & 71 & 78 & 83 & 87 & 95 & 103 & 112 & 121 & 121 & 120 & 111 & 101 & 92 \\ 61 & 69 & 78 & 82 & 87 & 90 & 93 & 100 & 108 & 109 & 111 & 111 & 112 & 106 & 100 & 100 \\ 72 & 82 & 92 & 94 & 95 & 97 & 98 & 105 & 112 & 106 & 100 & 102 & 103 & 101 & 99 & 97 \\ 84 & 82 & 106 & 94 & 104 & 97 & 104 & 105 & 117 & 106 & 90 & 102 & 95 & 101 & 98 & 98 \end{bmatrix}$$

(5.20)

These two quantization matrices will be used in quantizing order-4 and order-16 transform coefficients. To compare performance of the basic JPEG scheme and enhanced JPEG scheme using VBS technique, simulation is performed on monochrome images. The results are listed in Table 5.6 and Table 5.7. Fig.5.8 and Fig.5.9 show the images of LENNA and BABOON after being processed by the basic JPEG scheme and scheme 1 respectively.

By comparing Table 5.7 and Table 5.8, it can be seen that the application of VBS technique does not necessary produce MSE improvement. Also from Fig.5.8 and Fig.5.9, the blocking effects in scheme 1 coded images are more visible, particularly around those areas with uniform change. The reason is that these areas were coded using 16x16 block size but the order-16 quantization matrix is only derived using interpolation from the order-8 quantization matrix. The derived quantization values have not taken into consideration of the human visual effect and the noise is more visible in areas with uniform changes than in areas with high activities. Thus scheme 1 cannot give significant improvement over the basic JPEG scheme.

	LENNA			PEPPERS			SAILBOAT			BABOON		
Bit rate	1.00	0.75	0.50	1.00	0.75	0.50	1.00	0.75	0.50	1.00	0.75	0.50
MSE	34.6	48.8	73.7	35.7	48.6	74.8	97.9	129.9	191.8	304.2	370.7	459.0

Table 5.6 Simulation result for basic JPEG scheme.

Picture	LENNA			PEPPERS			SAILBOAT			BABOON		
Bit Rate	1.00	0.75	0.50	1.00	0.75	0.50	1.00	0.75	0.50	1.00	0.75	0.50
MSE	31.8	46.0	74.5	35.4	49.0	78.4	98.9	134.3	199.1	299.0	365.2	449.3

Table 5.7 Simulation Results for Scheme 1

(a) LENNA, 0.5 bpp

(d) BABOON, 0.5 bpp

(b) LENNA, 0.75 bpp

(e) BABOON, 0.75 bpp

(c) LENNA, 1.0 bpp

(f) BABOON, 1.0 bpp

Fig.5.8 Images after processed by basic JPEG scheme

(a) LENNA, 0.5 bpp

(d) BABOON, 0.5 bpp

(b) LENNA, 0.75 bpp

(e) BABOON, 0.75 bpp

(c) LENNA, 1.0 bpp

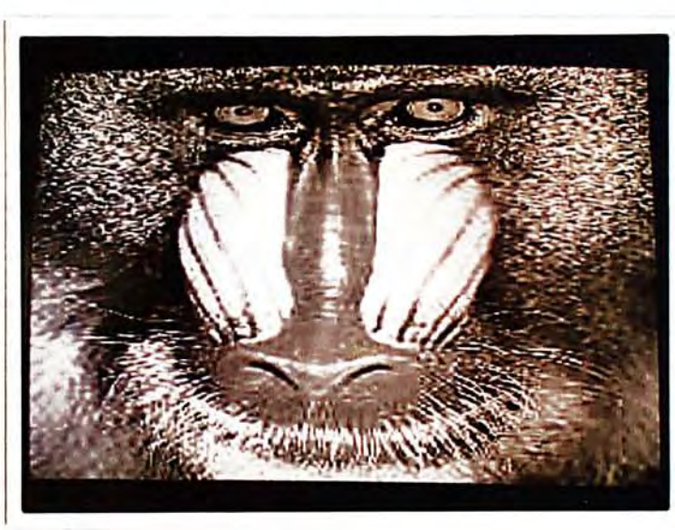

(f) BABOON, 1.0 bpp

Fig.5.9 Images after processed by scheme 1

5.4.2 Scheme 2

In scheme 1, by comparing Fig.5.8 and Fig.5.9, the problems seems mainly come from the blocks with size 16x16. So in scheme 2, we limit the block size to only 8x8 and 4x4. In other words, those with highest activity will be encoded as 4x4 blocks and those with medium or low activities will be encoded as 8x8 blocks. Other coding details are similar to those of scheme 1. Table 5.8 gives the MSE performance and Fig.5.10 shows the resulting images of LENNA and BABOON after being processed by scheme 2. The results shows that although there is some slightly improvement in reducing the blocking effect around those low activity blocks, the MSEs are even worse than that of scheme 1.

Picture	LENNA			PEPPERS			SAILBOAT			BABOON		
Bit Rate	1.00	0.75	0.50	1.00	0.75	0.50	1.00	0.75	0.50	1.00	0.75	0.50
MSE	32.5	47.8	80.1	34.2	48.2	83.2	96.6	133.5	208.6	304.2	371.5	468.7

Table 5.8 Simulation Results for Scheme 2

(a) LENNA, 0.5 bpp

(d) BABOON, 0.5 bpp

(b) LENNA, 0.75 bpp

(e) BABOON, 0.75 bpp

(c) LENNA, 1.0 bpp

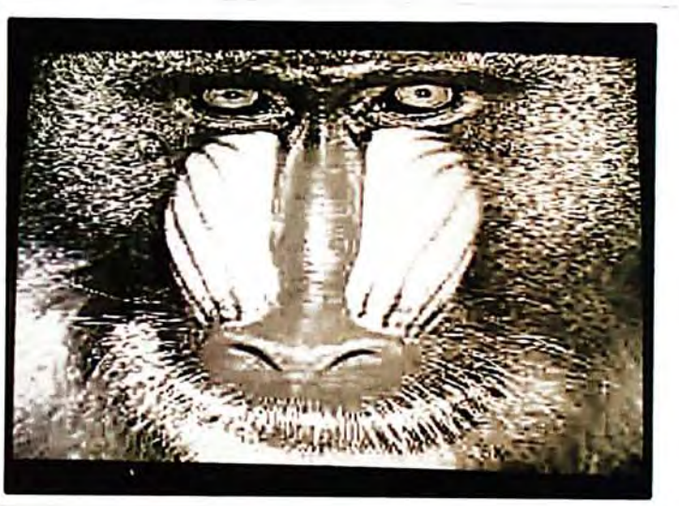

(f) BABOON, 1.0 bpp

Fig.5.10 Images after processed by scheme 2

5.4.3 Scheme 3

The major problem in scheme 1 is that the quantization matrix for N = 16 is obtained from that for N= 8. The resulting images, though have smaller MSE, produces larger blocking effect at those blocks with uniform change. The blocking effect may be due to the nonoptimum quantization matrices. In this scheme, we try to weight those elements of quantization matrix to see if there is chance to reduce the blocking effect. Fig.5.11 illustrate the methods used in weighting the quantization matrix.

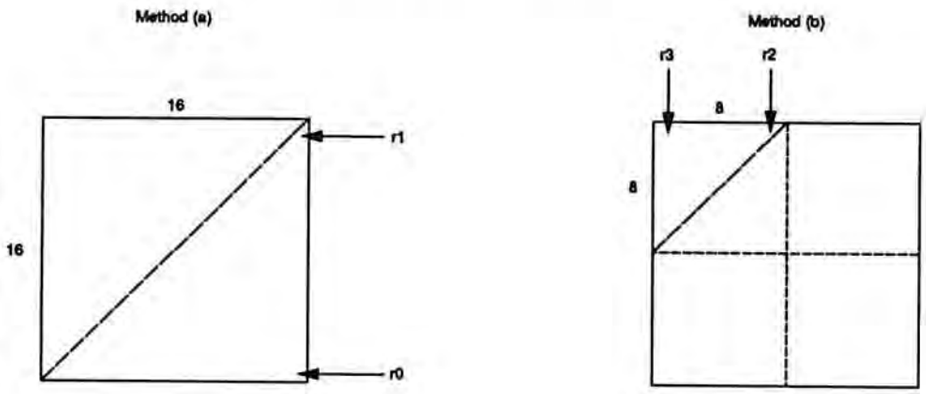

Fig 5.11 Illustration for the weighting factor

In method (a), the quantization values for higher sequency coefficients are weighted so that more bits are allocated to the high sequency coefficients of the 16x16 blocks. The $(u,v)^{th}$ quantization values, where $u+v < 15$, are unchanged. The highest sequency coefficient ($u = v = 15$) has its quantization value multiplied by r_0. For $(u,v) = (0,15)$ and $(u,v) = (15,0)$, their quantization values are multiplied by r_1. As more bits are to be allocated to higher sequency coefficients, we should have $r_0 < r_1 < 1$. For other $(u,v)^{th}$ quantization values, where $u+v \geq 15$, they are multiplied by a weighing factor r given by eq.(5.21) :

$$r = a\left(\frac{u+v}{30}\right) + b \qquad (5.21)$$

where $a = 2(r_0 - r_1)$, $b = 2r_1 - r_0$.

In method (b), the quantization values for lower sequency coefficients are weighted so that more bits are allocated to the low sequency coefficients of the 16x16 blocks. The $(u,v)^{th}$ quantization values, $u+v > 7$, are unchanged. The lowest sequency coefficient, (u,v) = (0,0), has its quantization value multiplied by r_3. For (u,v) = (0,7) and (u,v) = (7,0), their quantization values are multiplied by r_2. As more bits are to be allocated to lower sequency coefficients, we should have $r_3 < r_2 < 1$. For other $(u,v)^{th}$ quantization values, where $u+v \leq 7$, they are multiplied by a weighing factor r given by eq.(5.22) :

$$r = c\left(\frac{u+v}{14}\right) + d \qquad (5.22)$$

where $c = 2(r_2 - r_3)$, $d = r_3$.

Several sets of parameters, r_0,r_1, for subscheme S3.1-S3.2, and r_2,r_3 for subscheme S3.3-3.4 have been tested. The parameters are listed in Table 5.9 and the simulation results are given in Table 5.10.

Sub-scheme	r_0	r_1	r_2	r_3
S3.1	0.7	0.9	-	-
S3.2	0.5	0.7	-	-
S3.3	-	-	0.8	0.6
S3.4	-	-	0.9	0.6

Table 5.9 Parameters for sub-scheme.

Picture	LENNA			PEPPERS			SAILBOAT			BABOON		
Bit Rate	1.00	0.75	0.50	1.00	0.75	0.50	1.00	0.75	0.50	1.00	0.75	0.50
S3.1	31.3	45.5	76.0	36.4	50.4	83.7	101.8	139.9	211.9	299.8	365.5	454.4
S3.2	31.4	45.5	76.0	36.4	50.4	83.7	101.8	139.9	211.9	305.2	365.7	454.6
S3.3	31.7	45.5	74.7	36.9	50.5	82.1	103.1	139.2	206.7	304.4	367.9	451.6
S3.4	31.6	45.5	74.9	36.8	50.6	82.3	102.8	139.6	207.6	303.2	367.3	452.3

Table 5.10 Simulation Results for Scheme 3

It can be seen from Table 5.10 that although some sub-schemes give lower MSE, the improvement is still very little. Method (a) or scheme S3.1 and S3.2 seems give lower MSE performance when coded at 1.00 bpp and method (b) or scheme S3.3 - S3.4 seems give better MSE performance when coded at 0.5 bpp. However, all improvement is basically insignificant. Moreover, some even have no improvement at all. So this simple weighting of quantization value is not sufficient for improving the coding performance.

5.4.4 Scheme 4

Scheme 2,3,4 have been applied to monochrome images. In this scheme, we attempt to apply the VBS technique to colour images. After having colour space conversion by eq.(5.1), most information is concentrated in the Y component. To maintain the coding performance, the same coding method and block size of 8x8 in basic JPEG scheme is applied to the Y component. For the U,V components, they contain only auxiliary information and have more smooth changes. Larger distortion can be tolerated in coding U,V components without affecting the overall performance. Therefore, larger block size of 16x16 is used in coding the U,V components for larger bit rate reduction. In scheme 4, we set the block size for Y component equals to 8 and the block sizes for U,V components equal to 16.

To compare the performance of the scheme 4 with the basic JPEG scheme, simulation has been conducted and the results are shown in Table 5.11. The images of LENNA and BABOON, after being processed by scheme 4, are shown in Fig.5.12. By comparing Table 5.1 and Table 5.11, it can be seen that scheme 4 gives much lower MSE performance than the basic JPEG scheme. Comparison between Fig.5.6 and Fig.5.12 also shows that the visual quality of images after being processed by scheme 4 is better than those obtained by the basic JPEG scheme.

Picture	LENNA			PEPPERS			SAILBOAT			BABOON		
Bit Rate	1.00	0.75	0.50	1.00	0.75	0.50	1.00	0.75	0.50	1.00	0.75	0.50
MSE	77.6	95.0	126.8	127.9	154.0	206.0	251.3	296.1	379.1	507.1	572.0	660.2

Table 5.11 Simulation Results for JPEG Scheme, with $U_{size} = V_{size} = 16$

(a) LENNA, 0.5 bpp

(d) BABOON, 0.5 bpp

(b) LENNA, 0.75 bpp

(e) BABOON, 0.75 bpp

(c) LENNA, 1.0 bpp

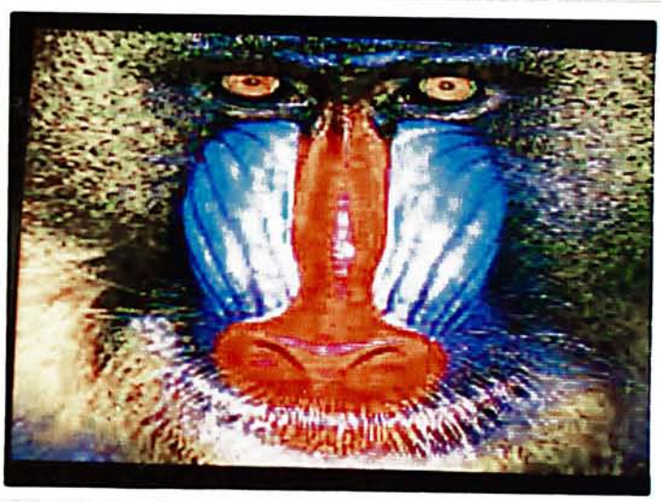

(f) BABOON, 1.0 bpp

Fig.5.12 Images after processed by scheme 4

5.4.5 Scheme 5

In scheme 4, the block size for luminance and chrominance components are 8x8 and 16x16 respectively. Better performance has been obtained by using larger block size for chrominance components. However, the predictor used for DC coefficients is still the previous element predictor. In section 5.3, we have proposed and demonstrated a more efficient MED predictor, which can substitute the previous element predictor. It can be expected that by combining both advantages of MED predictors and scheme 4, better performance can be obtained.

So, in this scheme, we apply the more efficient MED predictor for DC coefficients to scheme 4, both in luminance and chrominance components. The same coded images can be obtained as in scheme 4 and the MSE performance is shown in Table 5.12. It can be seen that in addition to the MSE improvement in scheme 4, we obtain a further bit rate reduction for the same coded images.

Picture	LENNA			PEPPERS			SAILBOAT			BABOON		
Bit Rate	0.971	0.727	0.483	0.976	0.731	0.487	0.985	0.738	0.493	0.993	0.744	0.495
MSE	77.6	95.0	126.8	127.9	154.0	206.0	251.3	296.1	379.1	507.1	572.0	660.2

Table 5.12 Simulation Results for JPEG Scheme, with $U_{size} = V_{size} = 16$, using MED predictor

5.4.6 Discussions and Conclusions

VBS technique and Edge Discriminator have been applied to the basic JPEG scheme. For monochrome images, the results of scheme 1, 2 and 3 show that there is no significant improvement in MSE performance and the blocking effect is more visible. The main reason may be due to the fact that order-4 and order-16 quantization matrices are derived from that of order-8. As the statistics and human visual sensitivity to transform coefficients of different order is not the same, the derived quantization matrices is far away from optimum and hence

there is not much improvement in coding performance of JPEG scheme using VBS technique. To obtain the advantage of VBS technique, therefore, some extensive experiments may be required to obtain the 4x4 and 16x16 quantization matrices that take into account of human visual system.

For colour images, we apply the VBS technique in a different manner. The block size for each Y,U,V are fixed, but are different between luminance (Y) and chrominance (U,V) components. As Y component contains the detail information about the images, the basic JPEG scheme with block size 8x8 is applied. Thus the advantage of the basic JPEG scheme is maintained in processing Y component. For U,V components, they contain less activities and so larger block sizes are more suitable. So the block size for U,V components can be set to 16x16 for larger bit rate reduction. The results show that with the same bit rate, the scheme with U,V components coded with block size 16x16 produce much smaller MSE performance.

Finally, the MED predictor described in section 5.3 is used for a further bit rate reduction. The results show that scheme 5, in which the block size are 8x8 and 16x16 for luminance and chrominance respectively, and MED predictor is used, both smaller MSE and lower bit rate can be obtained. Hence scheme 5 offers the best performance.

5.5 Conclusions

In this chapter, the basic JPEG scheme is studied. Two techniques have been used to enhance the performance of the basic JPEG scheme. The first one is by use of the MED predictor. This predictor is obtained by minimizing the edge differences between adjacent blocks. Simulation results show that the proposed MED predictor results in more precise prediction of DC coefficients. Among the predictors compared, the MED predictor requires the minimum number of bits to represent the DC coefficients. Its computation requires only low additional computation requirement and can maintain the simplicity of the basic JPEG

scheme. Moreover, the MED predictor uses information from previous adjacent blocks and requires only one-pass to perform the coding operation. Thus it can be easily incorporated into the basic JPEG scheme as an enhanced feature.

The other technique used is the VBS technique described in chapter 4. As images often have inhomogeneous activities over different areas, so the block size used to partition an image can be made adaptive. Monochrome and colour images have been tested using the VBS technique. For monochrome images, application of VBS technique cannot give improvement in both MSE and visual quality. The major reason is that the quantization matrix used for order-16 transform coefficients are derived from the quantization matrix for order-8 transform coefficients. No consideration has been given for the human visual sensitivities for different transform coefficients. Thus, the quantization matrices obtained are not optimum and the performance is not satisfactory. To obtain the benefit of VBS technique, therefore, extensive experiments taking into consideration of the human visual system, have to be conducted on finding the order-16 quantization matrices.

For colour images, a significant improvement in MSE have been obtained by using different block sizes for luminance and chrominance components. The block sizes used are 8x8 and 16x16 for luminance and chrominance components respectively. The visual quality of the coded images are better than those coded by the basic JPEG scheme. When combined with the MED predictor for encoding of the DC coefficients, a further bit rate reduction is obtained. This final scheme has the advantage that it maintains the simplicity of the JPEG scheme and remains a one-pass process. Both improvements in MSE and bit rate required are obtained. Therefore, this technique can be employed as an enhanced feature in the basic JPEG scheme.

6. CONCLUSIONS

6.1 Summary of Research Work

Transform coding of images has been used extensively in image data compression. Among various transforms, the DCT is mostly used because of its near optimum performance and existence of fast computational algorithm. However, the transform kernel components of the DCT are real numbers, which result in complex transformation process in a practical system. Dyadic Symmetry, proposed by CHAM in [CHAMc84], has been used for finding new transforms with simpler implementation but having not much degradation of coding performance. The same technique has also been used in generating new orthogonal Dyadic Matrices. In this thesis, the formation of Dyadic Matrices was examined. From the condition of orthogonality about the Dyadic Matrices, it has been found that the maximum size of Dyadic Matrix is 8. The relationship between destroying dyadic symmetry and Dyadic Matrix was discussed. Two examples of using these Dyadic Matrices in generating orthogonal transform for image coding were also given.

The DC coefficient truncation and restoration schemes for a transform coding system have been reported in [CHAMc84] [YIP88]. This method was further extended to low sequency coefficient truncation and restoration. By truncating more low sequency coefficients, it was expected that more bits will be allocated to high sequency coefficients for better visual quality of the coded images. Two schemes have been proposed but the results showed that the LSCT schemes cannot give improvement over the C&S scheme.

To take care of the inhomogeneous statistics over different areas of an image, block size used in a transform coding system needs to adapt to the local activities of an image. In this thesis, we examine a variable block size coding system proposed in [CHEN89] and

an Edge Discriminator was proposed to determine the block size. Simulations have been performed and the results showed that the VBS coding system using ED can give much performance improvement over that proposed by Chen.

After examining several techniques in transform coding, we studied the recently proposed JPEG scheme [JPEG90], which will become an international standard. In this thesis, we tried to enhance its performance using two techniques. Firstly, we used an more efficient MED predictor for DC coefficients. Simulation results showed that the MED predictor needs the minimum number of bits to represent the DC coefficients among all predictors tested. Secondly, the use of variable block size technique in the basic JPEG scheme was investigated. Five schemes using VBS technique were proposed and examined. It was found that scheme 5, in which block sizes of 8x8 and 16x16 are used for luminance and chrominance components respectively, and MED predictors are employed, can give much performance improvement in both MSE and visual quality over that of the basic JPEG scheme.

6.2 Contributions of Work

The main contributions of this project are summarized in the following four points :

1. The development of Dyadic Matrices was examined and it has been found that the maximum size of Dyadic Matrix is 8. The relationship between destroying dyadic symmetry as well as applying Dyadic Matrices to generate orthogonal transforms were also given.

2. Two Low Sequency Coefficient Truncation schemes were proposed and the problems in LSCT schemes were identified.

3. An Edge Discriminator was proposed to be used in a variable block size coding system. It can be used as a criterion in determining block size.

4. The basic JPEG scheme was examined. To enhance the performance, a MED predictor was proposed for encoding the DC coefficients. The variable block size technique using the Edge Discriminator have also been applied to the basic JPEG scheme to enhance its performance. By simulation, it was shown that a scheme 5, in which the MED predictor was employed and the block sizes for luminance and chrominance components were set differently, can enhance the performance of the basic JPEG scheme.

6.2 Suggestions for Further Research

In this project, there are still some areas in which further research can be performed for improvement. They are summarized as follow :

1. The development of Dyadic Matrices and the matrix order limitation have been shown. Further effort can be put in finding order-8 Dyadic Matrices that can be used to replace DCT in a transform coding system.

2. In LSCT scheme, it is found that the estimation error for low sequency coefficients should be sent to receiver. This can avoid error accumulation due to quantization and truncation of high sequency coefficients. However, the error transmission increases the bit rate. So effort can be put in finding more effective way in sending the error for bit rate reduction.

3. In enhancing the performance of the basic JPEG scheme, applying the VBS technique to monochrome image is not satisfactory. One of the reason is the non-optimum quantization matrix for order-16 transform coefficients. Further research can be done to obtain the quantization matrix, subject to human visual sensitivity and objective criterion, for performance improvement.

7. REFERENCES

[AHMEDtr74] Ahmed,N., T.Natarajan, Rao,K.R., 'Discrete Cosine Transform', *IEEE Trans. Comput.*, vol.23, pp.90-93, Jan. 1974

[AHMEDr75] Ahmed,N., and Rao,K.R., *Orthogonal Transforms for Digital Signal Processing*, Springer-Verlag, 1975.

[ANDREp68] Andrews,H.C. and Pratt,W.K., 'Fourier Transform Coding of Images', Hawaii International Conf. on System Sciences, pp.677-679, Jan. 1968.

[BRAINp90] R.C. Brainard and A. Puri, 'Compact Coder for Component Color Television', *IEEE Trans. Commun.*, vol.38, pp.223-232, Feb. 1990.

[CHAMac84] W.K. Cham, D.Allott and R.J.Clarke, 'Block Classification Image Coding with Combined Transforms', *Proc. of 1984 IEEE Conference on ASSP*, San Diego, California, USA, vol.2, pp.29.101-104, March 1984.

[CHAMc84] W.K. Cham and R.J. Clarke, 'DC Coefficient Restoration in Transform Image Coding', *IEE Proc.*, vol.131, part F, pp. 709-713, Dec. 1984.

[CHAMc86] Cham,W.K., and Clarke,R.J., 'Application of the Principle of Dyadic Symmetry to the Generation of Orthogonal Transforms', *IEE Proc.*, vol.133, pt.F, No.3, pp.264-270, June 1986.

[CHAM89] Cham,W.K., 'Development of Integer Cosing Transforms by the Principle of Dyadic Symmetry', *IEE Proc.*, vol.136, pt.1, No.4, pp.276-282, Aug. 1989.

[CHAM90] Cham,W.K., 'Formation of Dyadic Matrices using Dyadic Symmetry', unpublished report, 1990.

[CHAMc91] Cham,W.K., and Chan,Y.T., 'An Order-16 Integer Cosine Transform', *IEEE Trans. ASSP*, vol.39, pp.1205-1208, May 1991.

[CHENs77] Chen,W.H., and Smith,C.H., 'Adaptive Coding of Monochrome and Colour Images', *IEEE Trans. Commun.*, vol.25, pp.1285-1292, Nov.1977.

[CHENp84] Chen,W.H. and Pratt,W.K., 'Scene Adaptive Coder', *IEEE Trans. Commun.*, vol.32, pp.225-232, March 1984.

[CHEN89] Cheng-Tie CHEN, 'Adaptive Transform Coding Via Quadtree-Based Variable Blocksize DCT', *International Conference on ASSP*, pp.1854-1857, 1989.

[CLARK85] Clarke,R.J., *Transform Coding of Images*, Academic Press, 1985.

[CUBE90] 'Preliminary Data Book of CL550A JPEG Image Compression Processor', C-Cube Microsystems, Feb. 1990.

[ELSEV90] Elsevier, 'Draft Revision of Recommendation H.261 : Video Codec For Audiovisual Services at p x 64 kbit/s', *Signal Processing*, vol.2, no.2, pp.221-239, August 1990.

[JAIN79] Jain,A.K., 'A Sinusoidal Family of Unitary Transforms', *IEEE Trans. PAMI-1*, no.4, pp.356-365, Oct.1979.

[JAIN81] Jain,A.K., 'Image Data Compression : A Review', *Proc. IEEE*, vol. 69, no.3, pp.349-389, Mar. 1981.

[JAIN89] Jain,A.K., *Fundamentals of Digital Image Processing*, Prentice-Hall International, Inc., 1989.

[JPEG90] 'JPEG Technical Specification, Revision 5', *JPEG-8-R5*, Jan.1990.

[JURGE91] Ronald K. Jurgen, 'The Challenges of Digital HDTV', *IEEE Spectrum*, pp.28-30, pp.71-73, April 1991.

[MAX60] J.Max, 'Quantizing for Minimum Distortion', *IRE Trans IT*, vol.6, pp.7-12, 1960.

[NETRAl80] A.N. Netravali and J.O. Limb, 'Picture Coding : A Review', *Proc. IEEE*, vol.68, no.3, pp. 366-406, Mar. 1980.

[NGAN82] Ngan,K.N., 'Adaptive Transform Coding of Video Images', *IEE Proc.*, vol.129, pt.F, No.2, pp.28-40, Feb. 1982.

[NGANls89] Ngan,K.N., Kin S.Leong and H.Singh, 'Adaptive Cosine Transform Coding of Images in Perceptual Domain', *IEEE Trans. ASSP*, vol.37, no.11, pp.1743-1750, Nov. 1989.

[PRATTk69] Pratt,W.K. and Kane,J., 'Hadamard Transform Image Coding', *Proc.IEEE*, vol.57, no.1, pp.58-68, Jan.1969.

[REINIg83] Randall C.Reininger and Jerry D.Gibson, 'Distribution of the Two-Dimensional DCT Coefficients for images', *IEEE Trans. Comm.*, vol.31, no.6, pp.835-839, June 1983.

[SEElc91] See,C.T., Lo,K.T., and Cham,W.K., 'Efficient Encoding of DC Coefficients in Transform Coding of Images Using JPEG scheme', *Proc. 1991 IEEE International Symposium on Circuits and Systems*, pp.404-407, Singapore, June 1991.

[SEEc91] See,C.T. and Cham,W.K., 'An Adaptive Variable Block Size DCT Transform Coding System', *Proc. China 1991 International Conference on Circuits and Systems*, pp.305-308, Shenzhen, China, June 1991.

[TASTOw71] Tasto,N. and Wintz,P.A., 'Image Coding of Adaptive Block Quantization', *IEEE Trans. Comm. Tech.*, vol.19, no.6, pp.957-971, Dec. 1971.

[VAISEg87] D.Jacques Vaisey and Allen Gersho, 'Variable Block-Size Image Coding', *Proc. 1987 ICASSP*, Dallas/TX, pp.25.1.1-4, April 1987.

[WANGh84] Wang Zhongde and B.R.Hunt, 'Comparative Performance of Two Different Versions of the Discrete Cosine Transform', *IEEE Trans. ASSP*, vol.32, no.2, pp.450-453,

[YIP88] Yip,P.C., 'Transform Coding of Image', *M.Phil. Thesis*, Department of Electronics, The Chinese University of Hong Kong, May 1988.